The effects and mechanisms of action of TC-G 1008, GPR39 agonist, in animal models of seizures and epilepsy

Urszula Doboszewska (urszula.doboszewska@umcs.lublin.pl)
Maria Curie-Sklodowska University: Uniwersytet Marii Curie-Sklodowskiej https://orcid.org/0000-0002-2700-8155

Katarzyna Socala
Maria Curie-Sklodowska University: Uniwersytet Marii Curie-Sklodowskiej

Mateusz Pieróg
Maria Curie-Sklodowska University: Uniwersytet Marii Curie-Sklodowskiej

Dorota Nieoczym
Maria Curie-Sklodowska University: Uniwersytet Marii Curie-Sklodowskiej

Jan Sawicki
Medical University of Lublin: Uniwersytet Medyczny w Lublinie

Małgorzata Szafarz
Jagiellonian University: Uniwersytet Jagiellonski w Krakowie

Kinga Gaweł
Medical University of Lublin: Uniwersytet Medyczny w Lublinie

Anna Rafalo-Ulińska
Institute of Pharmacology of the Polish Academy of Sciences: Instytut Farmakologii im Jerzego Maja Polskiej Akademii Nauk

Adam Sajnóg
Adam Mickiewicz University: Uniwersytet Adama Mickiewicza w Poznaniu

Elżbieta Wyska
Jagiellonian University: Uniwersytet Jagiellonski w Krakowie

Camila V. Esguerra
University of Oslo: Universitetet i Oslo

Bernadeta Szewczyk
Institute of Pharmacology of the Polish Academy of Sciences: Instytut Farmakologii im Jerzego Maja Polskiej Akademii Nauk

Marzena Maćkowiak
Institute of Pharmacology of the Polish Academy of Sciences: Instytut Farmakologii im Jerzego Maja Polskiej Akademii Nauk

Danuta Barałkiewicz

Adam Mickiewicz University: Uniwersytet Adama Mickiewicza w Poznaniu

Katarzyna Młyniec

Jagiellonian University: Uniwersytet Jagiellonski w Krakowie

Gabriel Nowak

Institute of Pharmacology of the Polish Academy of Sciences: Instytut Farmakologii im Jerzego Maja Polskiej Akademii Nauk

Ireneusz Sowa

Medical University of Lublin: Uniwersytet Medyczny w Lublinie

Piotr Wlaź

Maria Curie-Sklodowska University: Uniwersytet Marii Curie-Sklodowskiej

---

Research Article

Keywords: GPR39, TC-G 1008, seizure, epilepsy, zinc, CREB

Posted Date: July 12th, 2022

DOI: https://doi.org/10.21203/rs.3.rs-1182423/v2

The effects and mechanisms of action of TC-G 1008, GPR39 agonist, in animal models of seizures and epilepsy

Urszula Doboszewska[1*], Katarzyna Socała[1], Mateusz Pieróg[1], Dorota Nieoczym[1], Jan Sawicki[2], Małgorzata Szafarz[3], Kinga Gaweł[4], Anna Rafało-Ulińska[5], Adam Sajnóg[6], Elżbieta Wyska[3], Camila V. Esguerra[7], Bernadeta Szewczyk[5], Marzena Maćkowiak[8], Danuta Barałkiewicz[6], Katarzyna Młyniec[9], Gabriel Nowak[5,9], Ireneusz Sowa[2], Piotr Wlaź[1]

[1]Department of Animal Physiology and Pharmacology, Institute of Biological Sciences, Maria Curie-Skłodowska University, Akademicka 19, PL 20-033 Lublin, Poland

[2]Department of Analytical Chemistry, Medical University of Lublin, Chodzki 4A, PL 20-093 Lublin, Poland

[3]Department of Pharmacokinetics and Physical Pharmacy, Jagiellonian University Medical College, Medyczna 9, PL 30-688 Kraków, Poland

[4]Department of Experimental and Clinical Pharmacology, Medical University of Lublin, Jaczewskiego 8b, 20-090 Lublin, Poland

[5]Department of Neurobiology, Maj Institute of Pharmacology, Polish Academy of Sciences, Smetna 12, PL 31-343 Krakow, Poland

[6]Department of Trace Analysis, Adam Mickiewicz University, Uniwersytetu Poznanskiego 8, 61-614 Poznan, Poland

[s7]Chemical Neuroscience Group, Centre for Molecular Medicine Norway, University of Oslo, Gaustadalléen 21, Forskningsparken, 0349 Oslo, Norway

[8]Laboratory of Pharmacology and Brain Biostructure, Department of Pharmacology, Maj Institute of Pharmacology, Polish Academy of Sciences, Smetna 12, PL 31-343 Krakow, Poland

[9]Department of Pharmacobiology, Jagiellonian University Medical College, Medyczna 9, PL 30-688 Kraków, Poland

*Corresponding author: Department of Animal Physiology and Pharmacology, Institute of Biological Sciences, Faculty of Biology and Biotechnology, Maria Curie-Sklodowska University, Akademicka 19, PL 20-033 Lublin, Poland. Phone: +48 81 537-50-10, Fax: +48 81 537-59-01; E-mail address: urszula.doboszewska@umcs.lublin.pl (U. Doboszewska); Present address: Department of Pharmacobiology, Jagiellonian University Medical College, Kraków, Poland, e-mail address: urszula.doboszewska@uj.edu.pl

ORCID identifiers:

Urszula Doboszewska: 0000-0002-2700-8155

Katarzyna Socała: 0000-0001-7706-2080

Mateusz Pieróg: 0000-0001-8772-3225

Dorota Nieoczym: 0000-0002-9446-7343

Jan Sawicki: 0000-0002-5945-1047

Małgorzata Szafarz: 0000-0002-8619-5659

Kinga Gawel: 0000-0001-8857-847X

Anna Rafalo-Ulińska: 0000-0001-7576-8039

Adam Sajnóg: 0000-0002-7385-2875

Elżbieta Wyska: 0000-0002-4798-0574

Camila V. Esguerra: 0000-0002-2271-8094

Bernadeta Szewczyk: 0000-0002-6863-7951

Marzena Maćkowiak: 0000-0002-6056-9595

Danuta Barałkiewicz: 0000-0002-1186-3552

Katarzyna Mlyniec: 0000-0002-9257-8154

Gabriel Nowak: 0000-0002-3000-7938

Ireneusz Sowa: 0000-0001-9346-6325

Piotr Wlaź: 0000-0002-5389-0241

Abstract

Extracellular/intracellular zinc ions are implicated in processes underlying seizures/epileptogenesis. The G-protein coupled receptor 39 (GPR39) was suggested as a target for extracellular zinc. Activation of GPR39 was proposed as a novel strategy for treating seizures but there was a paucity of data on the relationship between the function of this receptor and epileptogenesis. Furthermore, TC-G 1008, GPR39 agonist, has been increasingly used to study the function of GPR39 but it has not been validated in the GPR39 knockout setting. We found that the concentration of TC-G 1008 attained in the brain tissue following its i.p. administration in mice was sufficient to occupy GPR39. TC-G 1008 decreased the seizure threshold in the maximal electroshock seizure threshold test, but it increased the seizure threshold in the 6-Hz induced seizure threshold test. The compound increased the mean duration of EEG discharges in response to pentylenetetrazole (PTZ) in zebrafish larvae and facilitated the development of epileptogenesis in a chronic, PTZ-induced kindling model of epilepsy in mice. Using GPR39 knockout mouse line, generated by the CRISPR-Cas-9 method, we demonstrated that GPR39 is target for TC-G 1008 regarding PTZ-induced epileptogenesis. However, a concomitant analysis of the downstream effects on cyclic-AMP-response element binding protein in GPR39 knockout mice suggested that TC-G 1008 also acts via other targets. Conclusion and implications: Our data argue against GPR39 activation being a viable therapeutic strategy for treating epilepsy. They also suggest that investigations need to consider whether TC-G 1008 is indeed a selective agonist of the GPR39 receptor.

Keywords: GPR39, TC-G 1008, seizure, epilepsy, zinc, CREB

Introduction

Most of zinc ions are bound to proteins but the small pool of "free" or "labile" zinc is available for signaling, which occurs both intracellularly and extracellularly (Maret 2017). Although studies did not provide direct intracellular/extracellular concentrations of zinc ions associated with seizures (Doboszewska et al. 2019), a link between increased intracellular "free" zinc concentration ($[Zn^{2+}]_I$) and status epilepticus (SE), which is a risk factor for epilepsy (Fountain 2000), was demonstrated (van Loo et al. 2015). Furthermore, an association between $[Zn^{2+}]_I$ and metal regulatory transcription factor 1 (MTF1), a candidate $[Zn^{2+}]_I$ sensor (Carpenter and Palmer 2017), was depicted in an animal model of SE and in human hippocampi surgically resected from patients with pharmacoresistant form of the disease. The neuromodulatory function of extracellular zinc on numerous targets that mediate neuronal excitation or inhibition was shown to be of importance in terms of seizures/epilepsy (Doboszewska et al. 2019). Moreover, extracellular zinc was suggested to activate a G-protein-coupled receptor (GPCR), namely GPR39 (Holst et al. 2007; Yasuda et al. 2007). The existence of a GPCR activated by zinc ions was postulated before (Hershfinkel et al. 2001) although there is still debate whether the physiological/ pathophysiological concentrations of zinc are sufficient to activate the receptor (Maret 2001) and whether it is a real agonist or a neuromodulator.

Despite the controversies surrounding the endogenous ligand, as a receptor belonging to "druggable" GPCRs (Hauser et al. 2017), the GPR39 receptor is gaining increasing attention as a target for future drugs in different therapeutic areas (Iovino et al. 2022; Methner et al. 2021), including the central nervous system (Davis et al. 2021; Sah et al. 2021; Xie et al. 2021). Data indicated the association between the function of GPR39 receptor and seizures. GPR39 knockout (KO) mice displayed enhanced susceptibility to seizures triggered by a single intraperitoneal (*i.p.*) injection of kainic acid (KA), compared with wild-type (WT) littermates

(Gilad et al. 2015). Lithium chloride-pilocarpine-induced-SE decreased the expression of GPR39 at the protein level in the hippocampus (Chen et al. 2019). RNA sequencing revealed up-regulation of the *gpr39* gene in *stim2b* knockout zebrafish, which is hyperactive and more sensitive to treatment with pentylenetetrazole (PTZ) (Wasilewska et al. 2020). The role of GPR39 gene in the process of epilepsy development, *i.e.*, epileptogenesis (Galanopoulou et al. 2012) has not been examined.

In contrast to a seizure, which is a transient occurrence of signs and/or symptoms due to abnormal, excessive, or synchronous neuronal activity in the brain, and can be induced temporarily, epilepsy is a brain disease characterized by an enduring predisposition to generate seizures (Fisher et al. 2014; Goldberg and Coulter 2013). Thus, exploration of the basis of epileptogenesis is of utmost importance because. Furthermore, as epilepsy is a heterogeneous group of neurological diseases with different etiologies and no single model reflects key features of epilepsy(epilepsies), the use of multiple models of seizures/ epileptogenesis is necessary to study their pathophysiology/ pharmacology (Loscher 2021).

We hypothesized that activation of the GPR39 receptor may reduce seizures and/or produce an antiepileptogenic effect. We utilized a small molecule agonist at the GPR39 receptor, TC-G 1008 and the nonspecific agonist, zinc chloride ($ZnCl_2$). TC-G 1008 (compound 3 (Peukert et al. 2014), GPR39-C3 (Sato et al. 2016)) is a positive allosteric modulator which activated cAMP production (downstream of Gs), IP1 accumulation (downstream of Gq), SRF-RE-dependent transcription (downstream of G12/13), and β-arrestin recruitment (Peukert et al. 2014). Similarly, zinc stimulated signaling at GPR39 via G_s, G_q, $G_{12/13}$ and β-arrestin pathways (Holst et al. 2007). Importanly, since its discovery TC-G 1008 has been broadly used in investigations and its effects were translated to the effects of GPR39 receptor activation, but the compound has not been validated in the GPR39 KO setting (Laitakari et al. 2021).

We first compared the effects induced by GPR39 agonists (TC-G 1008, $ZnCl_2$) to that of a standard antiseizure drug, valproic acid (VPA) in a variety of acute seizure tests or a chronic model reflecting epileptogenesis. Our aim was to assess their behavioral or electroencephalographic (EEG) effects. We also generated GPR39 KO mice to assess their response to seizure-inducing/ epileptogenic agents and the treatment with TC-G 1008, thus gaining more insights into the phenotype of GPR39 KO mice and the role of the GPR39 gene. This experiment allowed us to determine whether the GPR39 receptor is a target for TC-G 1008 in the selected animal model. Then, we examined whether the effects of TC-G 1008 or GPR39 KO are accompanied by alterations in different pools of zinc (including total zinc and $[Zn^{2+}]_I$) in serum and hippocampus, a region of the brain important in terms of epileptogenesis (Thom 2014). Finally, we investigated the expression of proteins of the GPR39 signaling pathway in the hippocampi of mice subjected to the above-mentioned models of seizures or epilepsy. The latter analysis performed in hippocampal samples obtained from GPR39 KO mice showed that TC-G 1008 may act non-selectively.

Methods

Materials

TC-G 1008 was purchased from Adooq Bioscience LLC (Irvine, CA, USA). VPA (sodium salt), $ZnCl_2$, PTZ and KA were obtained from Sigma-Aldrich. For experiments in mice, $ZnCl_2$, VPA, PTZ and KA were dissolved in physiological saline (0.9% sodium chloride (NaCl) solution). TC-G 1008 was suspended in 1% Tween 80 solution in physiological saline. For experiments in zebrafish, $ZnCl_2$ and TC-G 1008 were dissolved in embryo medium. PTZ was dissolved to 60 mM (3x stock) in embryo medium. The materials used for biochemical analyses are listed in the sections on Liquid Chromatography Tandem Mass Spectrometry (LC-MS/MS), Western blot, Inductively Coupled Plasma Optical Emission Spectrometry (ICP-OES), Laser Ablation Inductively Coupled Plasma Mass Spectrometry (LA-ICP-MS) or Zinpyr-1 (ZP-1) staining.

Animals

The experiments were performed in non-genetically modified mice, GPR39 KO mice and in zebrafish (*Danio rerio*) larvae. Housing and experimental procedures were conducted in accordance with the European Union Directive of 22 September 2010 (2010/63/EU), and Polish and Norwegian legislation acts concerning animal experimentation. The experiments in mice were approved by the Local Ethical Committee in Lublin (experiments in non-genetically modified mice: approval numbers 38/2017, 48/2018, 110/2018, 36/2019; experiments in GPR39 KO mice: approval numbers 72/2019, 16/2020), and the I Local Ethical Committee in Warsaw (approval number 811/2019 regarding generation of the GPR39 KO mouse line). The experiments in zebrafish were approved by the Norwegian Food Safety Authority experimental animal administration's supervisory and application system (“Forsøksdyrforvatningen tilsyns- og søknadssystem”; FOTS ID 15469 and 23935). All

efforts were made to minimize animal suffering as well as the number of animals used in the study. During the experiments, the animals were closely followed-up by the animal caretakers and researchers, with regular inspection by a veterinarian, according to the standard health and animal welfare procedures of the local animal facility.

Experimentally naïve male Swiss Albino mice (n=966) with a body weight range of 17–31 g, were purchased from a licensed breeder (Laboratory Animals Breeding, Ilkowice, Poland) and were housed in an animal house at the Faculty of Biology and Biotechnology of Maria Curie Sklodowska University in Lublin, in groups of 7-8 in open Makrolon cages (37 cm × 21 cm × 14 cm) under strictly controlled laboratory conditions (temperature maintained at 21–24 °C, relative humidity at 45–65%) with an artificial 12/12 h light/dark regime (light on at 6:00 a.m.). A rodent chow diet (Murigran, Agropol S.J., Motycz, Poland) and tap water were provided *ad libitium*. The environment was enriched with nest material and paper tubes.

GRP39 KO mouse model was generated by the Mouse Genome Engineering Facility (crisprmice.eu). A CRISPR/Cas 9 method was used to establish the model in mixed genetic background (C57BL/6/Tar x CBA/Tar). A deletion of 44 bp causing p.Lys38fs*57X frameshift mutation was introduced. WT and KO mice were housed in an animal house at the Experimental Medicine Center of the Medical University in Lublin. Male WT mice (n=35) and male KO mice (n=35) with a body weight range of 16-29 g were used for experiments. The mice were housed in groups of 7-8 in open Makrolon cages (37 cm × 21 cm × 14 cm) under strictly controlled laboratory conditions (temperature maintained at 21–24 °C, relative humidity at 45–65%) with an artificial 12/12 h light/dark regime (light on at 6:00 a.m.). The diet (Altromin standard diet, Altromin, Lage, Germany) and tap water were provided *ad libitium*. The environment was enriched with nest material and paper tubes. Only male Swiss Albino or C57BL/6/Tar x CBA/Tar mice were used to exclude the possible impact of the estrous cycle on seizure susceptibility (Socala and Wlaz 2021).

The following procedures were performed in Swiss Albino mice: determination of TC-G 1008 concentration in serum and brain, maximal electroshock seizure (MES) threshold test (MEST), MES generated by supramaximal stimulus of 50 mA, 6-Hz-induced seizure threshold test, 6-Hz seizure generated by supramaximal current intensity of 32 mA, intravenous (*i.v.*) PTZ seizure threshold test, acute KA-induced seizures, PTZ kindling and biochemical analyses. The following procedures were performed in C57BL/6/Tar x CBA/Tar GPR39 KO and WT mice: the MEST test, PTZ kindling and biochemical analyses. Animals were randomly assigned to the experimental groups. Blinding was not feasible during behavioral experiments due to the rotations of experimenters who either administered compounds or observed their behavioral effects. Blinding was applied during biochemical analyses.

All procedures in mice begun after at least one week of acclimatization and were performed between 8:00 a.m. to 3:00 p.m., after a minimum 30-min adaptation period to the conditions in the experimental room. Drug solutions/suspensions were prepared freshly and administered i.p. at a volume of 0.1 ml per 10 g of body weight. Control groups received vehicles (VEH) used for the preparation of drug solutions/suspensions. The drugs were administered 30 min before acute seizure tests or acute seizure models or before PTZ/KA injections. This pretreatment time was chosen after determination of TC-G 1008 concentrations in serum and brain (Fig 1). With the exception of 1% ophtalmic solution of tetracaine, which was used for a short-term topical ophthalmic anesthesia before determining the seizure thresholds or performing MES or 6-Hz seizure, no anesthetics or analgesics were used, to reduce the possibility of a pharmacodynamic or pharmacokinetic interaction between these agents and the examined compounds. Each animal was used only once in acute seizure test. Following acute seizure tests, the surviving mice were euthanized by >70% carbon dioxide (CO_2) or by cervical dislocation by a person trained for this procedure.

Adult zebrafish (*Danio rerio*) stocks of AB strain (Zebrafish International Resource Center, Oregon, USA) were maintained at standard aquaculture conditions, i.e., 28.5˚C, on a 14/10 h light/dark cycle in 8.0 L tanks [27 cm long, 21 cm wide and 17 cm high]. Fertilized eggs were collected via natural spawning. Embryos were reared under constant light conditions in embryo medium, i.e., Danieu's buffer: 1.5 mM Hepes, pH 7.6, 17.4 mM NaCl, 0.21 mM KCI, 0.12 mM $MgSO_4$ and 0.18 mM $Ca(NO_3)_2$. All embryos and larvae were kept in incubator, at 28.5˚C. The maximum tolerated concentration was evaluated in n=144 larvae of 4 days post-fertilization (dpf). For EEG experiments, n=80 larvae of 6 dpf were used.

Maximal electroshock seizures

MES induced seizure is among the most widely used rodent models of acute seizure (Socala and Wlaz 2021). 1% ophtalmic solution of tetracaine was administered for a short-term topical ophthalmic aneasthesia. Then, constant current stimuli (sine-wave pulses at 50 Hz for 200 ms) were applied *via* saline-soaked transcorneal electrodes with the usage of rodent shocker (type 221; Hugo Sachs Elektronik, Freiburg, Germany). During stimulation, mice were restrained manually and immediately following stimulation they were placed in a transparent box without bedding for behavioral observation on the presence or absence of seizure activity. Tonic hindlimb extension, defined as the rigid extension of the hindlimb that exceeds a 90° angle with the body, was considered as an endpoint.

Two experimental approaches were used: (1) the MEST test that employed stimulation at varied current intensities (7.6–17.4 mA) and (2) MES that employed stimulation at a fixed current intensity (50 mA). The mice were injected with a single dose of TC-G 1008, $ZnCl_2$, VPA or VEH (1% Tween 80 solution in physiological saline). 30 min later the MEST test was performed. The threshold current was established according to an 'up-and-down' method described by Kimball et al. (1957). Current intensity was lowered or raised by 0.06-log intervals

depending on whether the previously stimulated animal did or did not exert tonic hindlimb extension, respectively. The data obtained in groups of 20 animals were used to determine the threshold current causing endpoint in 50% of mice (CS_{50} with confidence limits for 95% probability). In the MEST test, the dose-response relationship was assessed. An initial dose of TC-G 1008 or $ZnCl_2$ was selected and the dose was either increased or decreased in a subsequent group of mice, depending on whether the previous dose affected the seizure threshold. The dose of VPA has been established to increase seizure threshold in this test (Socala et al. 2018). Following MEST, the mice were euthanized by >70% carbon dioxide (CO_2).

Groups of mice (n=10) were injected with a single dose of TC-G 1008, $ZnCl_2$, VPA or VEH. 30 min later they were stimulated with supramaximal MES stimulus of 50 mA. The doses of drugs applied before MES were based on the results of the MEST test – either effective or ineffective doses of TC-G 1008 and $ZnCl_2$ were administered. Control, non-stimulated (sham) animals received the respective doses of drugs or VEH but did not receive MES stimulus.

Six hertz (6 Hz) seizures

The 6-Hz seizure model is another model of acute seizures which is required while screening for antiseizure drugs (Khanam and Vohora 2021). 1% ophtalmic solution of tetracaine was used for a short-term topical ophthalmic anaesthesia. Then, square-wave alternating current stimuli (0.2-ms duration pulses at 6 Hz for 3 s) were applied *via* saline-soaked transcorneal electrodes using a Grass model CCU1 constant current unit coupled to a Grass S48 stimulator (Grass Technologies, Warwick, RI, USA). Mice were manually restrained during stimulation. Immediately following the stimulation, mice were placed in a transparent box without bedding for behavioral observation. The 6-Hz seizures were characterized by stun (fixed) posture, rearing, forelimb clonus, twitching of the vibrissae, and elevated tail. Lack of

the features listed above or the resumption of normal exploratory behavior within 10 s after stimulation were considered as the absence of seizures.

Two experimental approaches were used: (1) the 6-Hz seizure threshold test that employed stimulation at varied current intensities (10.0–20.0 mA) and (2) the 6-Hz seizure which was induced by supramaximal stimulation at a fixed current intensity (32 mA). The mice were injected with a single dose of TC-G 1008, $ZnCl_2$, VPA or VEH (1% Tween 80 solution in physiological saline). 30 min later the 6-Hz seizure threshold test was performed. The current intensity values were established according to an 'up-and-down' method (Kimball et al. 1957). The animals were stimulated at current intensity that was lowered or raised by 0.06-log intervals depending on whether the previously stimulated animal did or did not respond with seizures, respectively. The data obtained in groups of 20 animals were used to determine the threshold current causing 6-Hz-induced seizures in 50% of mice (CS_{50} with confidence limits for 95% probability). In the 6-Hz threshold test, the dose-response relationship was assessed. An initial dose of TC-G 1008 or $ZnCl_2$ was selected and the dose was either increased or decreased in a subsequent group of mice, depending on whether the previous dose affected the seizure threshold. The dose of VPA has been established to increase seizure threshold in this test (Socala et al. 2018). Following the 6-Hz seizure threshold test, the mice were euthanized by >70% carbon dioxide (CO_2).

Groups of mice (n=8) were injected with a single dose of TC-G 1008, $ZnCl_2$ or VPA, which was effective in the 6-Hz threshold test, or VEH. 30 min later the mice were stimulated with supramaximal current intensity of 32 mA. Control, non-stimulated (sham) animals received the respective doses of drugs or VEH but did not receive the supramaximal current intensity of 32 mA.

Kainic acid-induced seizures

Groups of mice (n=8-12) were injected *i.p.* with a single dose of TC-G 1008, $ZnCl_2$ or VEH (1% Tween 80 solution in physiological saline). 30 min later the mice were injected *i.p.* with a single dose of KA (40 mg/kg) (Lee et al. 2000). Immediately following KA injection, mice were placed individually into a transparent box without bedding for 2 h for behavioral observation. Seizure severity of each mice was scored according to the modified Racine's scale: stage 0, no response; stage 1, immobility and staring; stage 2, scratching/myoclonic jerks; stage 3, forelimb clonus; stage 4, rearing; stage 5, rearing and falling; stage 6, jumping, circling, rolling; stage 7, status epilepticus, death (Cole et al. 2000; Iqbal et al. 2018; Lee et al. 2000). The dose-response relationship was assessed. An initial dose of TC-G 1008 or $ZnCl_2$ was selected and the dose was either increased or decreased in a subsequent group of mice, depending on whether the previous dose exerted a response. The surviving animals were immediately euthanized by >70% carbon dioxide (CO_2).

Intravenous pentylenetetrazole (PTZ) seizures

PTZ induced seizure is among the most widely used rodent models of acute seizure (Socala and Wlaz 2021). Groups of mice (n=9-12) were injected *i.p.* with a single dose of TC-G 1008, $ZnCl_2$, VPA or VEH (1% Tween 80 solution in physiological saline). 30 min later the mice were placed in the cylindrical plastic restrainer (12-cm long, 3-cm inner diameter). The lateral tail vein was catheterized with a 2-cm long 27-gauge needle attached by polyethylene tubing PE20RW (Plastics One Inc., Roanoke, VA, USA) to a 5-ml plastic syringe containing 1% aqueous solution of PTZ. The syringe was mounted on a syringe pump (model Physio 22, Hugo Sachs Elektronik–Harvard Apparatus GmbH, March-Hugstetten, Germany). The accuracy of needle placement in the vein was confirmed by appearance of blood in the tubing. The needle was secured to the tail by an adhesive tape. Following catheterization, mice were

released from the restrainer and placed in a Plexiglas arena for behavioral observation. The PTZ solution was infused at a constant rate of 0.2 ml/min. The time intervals from the commencement of PTZ infusion to the onset of each of three endpoints (the first myoclonic twitch, generalized clonus with loss of the righting reflex, and tonic forelimb extension) were recorded. The PTZ infusion was stopped at the beginning of tonic seizures, which were usually lethal for mice. All surviving animals were euthanized immediately by cervical dislocation. The seizure thresholds were calculated separately for each endpoint using the following formula: threshold dose of PTZ (mg/kg) = (infusion duration (s) × infusion rate (ml/s) × PTZ concentration (mg/ml))/body weight (kg) and were expressed as the dose of PTZ (in mg/kg) needed to produce the first apparent sign of each endpoint. The dose-response relationship was assessed. An initial dose of TC-G 1008 or $ZnCl_2$ was selected and the dose was either increased or decreased in a subsequent group of mice, depending on whether the previous dose affected the seizure threshold. The dose of VPA has been established to increase seizure threshold in this test (Socala et al. 2018). Data obtained in the *i.v.* PTZ seizure threshold test are presented as the amount of PTZ (in mg/kg) ± SEM needed to produce the first apparent sign of each endpoint in each experimental group.

PTZ kindling model

PTZ-kindling model in mice has been established as a model for epileptogenesis (Potschka 2021). The mice were injected *i.p.* with VEH (1% Tween 80 solution in physiological saline), TC-G 1008, $ZnCl_2$ or VPA on every alternate day. 30 min later, they were injected *i.p.* with a subthreshold dose of PTZ. The subthreshold doses of PTZ, which induce kindling phenomenon, range from 25 to 45 mg/kg (Potschka 2021). In the case of kindling in Swiss Albino mice, the dose of PTZ was 40 mg/kg, as determined in our previous study (Socala et al. 2019). In the case of kindling in C57BL/6/Tar x CBA/Tar mice, the dose of PTZ was 25 mg/kg,

as determined in our preliminary experiment. Immediately following PTZ injection, mice were placed individually into a transparent box without bedding for 30 min for behavioral observation. Seizure severity of each subject was scored using the modified Racine's scale: stage 0, no response; stage 1, immobility, ear and facial twitching; stage 2, myoclonic jerks; stage 3, forelimb clonus, stage 4, clonic seizure with rearing and falling; stage 5, generalized clonic seizure with loss of righting reflex; stage 6, tonic fore- and hindlimb extension (Socala et al. 2019). The mean seizure severity scores were calculated for all experimental groups after each PTZ injection. Control, non-kindled animals received the respective doses of drugs but were injected with physiological saline (SAL) instead of PTZ solution. PTZ kindling models were terminated to reduce potential mortality when any of the groups displayed consecutive stage 5 or 6 seizures. The group of Swiss Albino mice receiving TC-G 1008 and the WT group of C57BL/6/Tar x CBA/Tar mice receiving TC-G 1008 displayed the highest seizure score during respective PTZ kindling models. 15 Swiss Albino mice per group or 15 WT and 15 GPR39 KO mice were used in these models.

Grip-strength test

The effects of single doses of TC-G 1008, $ZnCl_2$ or VPA or repeated doses of these compounds and PTZ kindling on skeletal muscular strength were evaluated in Swiss Albino mice or C57BL/6/Tar x CBA/Tar mice using the grip-strength test (Socala et al. 2020). The grip-strength apparatus (BioSeb, Chaville, France) consisted of a steel wire grid (8 × 8 cm) connected to an isometric force transducer. The animal was lifted by its tail so that it could grasp the grid with its forepaws. The mouse was then gently pulled backward until it released the grid and the maximal force in newtons (N) exerted by the mouse before losing grip was measured. The procedure was repeated three times and the mean force exerted by each mouse

before losing grip was recorded. The mean force was then normalized to body weight and expressed in mN/g ± SE.

Chimney test

The effects of single doses of TC-G 1008, $ZnCl_2$ or VPA or repeated doses of these compounds and PTZ kindling on motor deficits were evaluated in Swiss Albino mice or C57BL/6/Tar x CBA/Tar mice using the chimney test (Socala et al. 2020). In this test, the inability of animals to climb back-ward up through a Plexiglas tube (3 cm, inner diameter × 30 cm, length) within 60 s was an indicator of motor impairment.

Toxicological assessment in zebrafish

The maximum tolerated concentration was evaluated prior further experiments in zebrafish laravae. Groups (n=12) of 4 dpf zebrafish larvae were incubated with a range of TC-G 1008 or $ZnCl_2$ doses at 28.5˚C for 18 hours. 6 doses of each compound (TC-G 1008 or $ZnCl_2$) were tested. The following parameters were scored after 2 and 18 h of exposure: touch response, posture, edema, morphology, signs of necrosis, swim bladder and heartbeat. The dose of 65 µM Zn and 70 µM TC-G 1008 were chosen for EEG experiments.

EEG discharges assessment in zebrafish

PTZ-induced acute seizure model in zebrafish larvae is well-validated in terms of predictive validity and allows one to assess EEGs (Afrikanova et al. 2013; Gawel et al. 2020). A single 6 dpf zebrafish larvae were placed in a 48-well plate (one larva per well) filled with 200 µl of VEH (embryo medium, i.e., Danieu's buffer: 1.5 mM Hepes, pH 7.6, 17.4 mM NaCl, 0.21 mM KCI, 0.12 mM $MgSO_4$ and 0.18 mM $Ca(NO_3)_2$), $ZnCl_2$ or TC-G 1008 solution. Subsequently, larvae were incubated for 20 h at 28.5˚C. After incubation, larvae were exposed

to VEH or 20 mM PTZ for 5 min. Thereafter, larvae were immobilized in a thin layer of 2% low-melting-point agarose and the glass electrode (resistance 1-5 MΩ) filled with artificial cerebrospinal fluid (124 mM NaCl, 2 mM KCl, 2 mM $MgSO_4$, 2 Mm $CaCl_2$, 1.25 mM KH_2PO_4, 26 mM $NaHCO_3$, 10 mM glucose) was placed into the optic tectum (MultiClamp 700B amplifier, Digidata 1550 digitizer, Axon instruments, USA) (Afrikanova et al. 2013; Nieoczym et al. 2019). Single recordings for each larva were performed for a period of 20 minutes. The discharges were analyzed according to the duration of spiking paroxysms and only those were taken into account when the amplitude exceeded three times the background noise. The data were analyzed with the aid of Clampfit 10.2 software (Molecular Devices Corporation, USA) and custom-written programme for R (Windows). For EEG discharges assessment, n=5-17 larvae per group were used.

Tissue processing for biochemical analysis

For LC-MS/MS analysis, the mice were killed by rapid decapitation at four time points (15, 30, 60 and 120 min) after *i.p.* injection of TC-G 1008. For Western blot, ZP-1 staining, ICP-OES analysis the mice were killed ca. 3 min after MES or 6-Hz seizure or 24 h after the completion of the kindling paradigm. For LA-ICP-MS analysis the mice were killed 24 h after the completion of the kindling paradigm. The brains were rapidly dissected and immersed in cooled (2-8°C) 0.9% NaCl solution. For LC-MS/MS analysis, the whole brains were frozen. For Western blot and ZP-1 staining, the brains were rapidly dissected on a cold plate into left and right hemispheres. Left hippocampi (dorsal and ventral) were dissected, immediately frozen on dry ice and stored at -80°C until Western blot analysis. The right hemispheres were frozen by liquid nitrogen and were stored at −80°C until cryo-sectioning. 12 µm hippocampal coronal sections were prepared from right hemispheres using cryostat microtome Leica CM 1850, Germany and were attached to glass slides (SuperFrost microscope slides, cut edges, Thermo

Scientific Menzel Glaser. The glass slides were stored at −80 °C until further analysis. The trunk blood was collected into tubes without anti-coagulant. The blood was allowed to clot for 15-20 min and then centrifuged for 10 min at 5600 rpm at 4°C. The resulting supernatant (serum) was pipetted into tubes that were stored at -80°C until LC-MS/MS or ICP-OES analysis. The biochemical analyses were performed by experimenters blinded for the treatment.

Determination of TC-G 1008 concentrations by LC-MS/MS

The concentrations of TC-G 1008 were determined in serum and brain of Swiss Albino mice 15, 30, 60 and 120 min after compound administration (20 mg/kg, *i.p.*), using the LC-MS/MS method. The brains were homogenized in distilled water (1:3, *w*/*v*) with a tissue homogenizer TH220 (Omni International, Inc., Warrenton, VA, USA). Purification of the samples was performed by protein precipitation procedure with 0.1% formic acid in acetonitrile containing pentoxifylline used as an internal standard (2000 ng/mL) added to the samples at the ratio of 1:2 (*v/v*). Then, the samples were shaken for 10 min (IKA Vibrax VXR, Germany) and after centrifugation (Minispin, Eppendorf, Germany) for 10 min at the 12 000 rpm the supernatant was transferred into autosampler vials. The HPLC system (Agilent 1100, Agilent Technologies, Waldbronn, Germany) consisted of a degasser, binary pump, column oven and an autosampler. Chromatographic separation was carried out on an XBridge™ C18 analytical column (3x50 mm, 5µm, Waters, Ireland) with the oven temperature set at 30°C. The autosampler temperature was maintained at 10°C and a sample volume of 15 µL was injected into the LC-MS/MS system. The mobile phase containing 0.1% formic acid in acetonitrile (A) and 0.1% formic acid in water (B) was set at a flow rate of 0.4 mL/min. Initial mobile phase composition was 95% B with a linear gradient to 30% B in the first 5 min, then isocratic mode for 5 min with the subsequent rapid change back to 95% B in 0.1 min. The remaining time of elution was set at 95% B. The whole HPLC operation lasted 13 min. Mass spectrometric

detection was performed on an Applied Biosystems MDS Sciex (Concord, Ontario, Canada) API 2000 triple quadrupole mass spectrometer equipped with an electrospray ionization (ESI) interface. ESI ionization in the positive ion mode was used for ion production. The tandem mass spectrometer was operated at unit resolution in the selected reaction monitoring mode (SRM), monitoring the transition of the protonated molecular ions *m/z* 419 to 305 and *m/z* 419 to 171 for compound TC-G 1008 (the first pair was used as a quantifier and the second pair was employed for the identity verification as a qualifier) and *m/z* 279 to 181 for the internal standard. The mass spectrometric conditions were optimized for TC-G 1008 by continuous infusion of the standard solution at the rate of 10 μL/min using a Harvard infusion pump. The ion source temperature was maintained at 400°C. The ionspray voltage was set at 5500V. The curtain gas (CUR) was set at 20 psi and the collision gas (CAD) at 12 psi. The optimal collision energy (CE) was 45V. The following parameters of ion path were used as the most favorable ones: declustering potential (DP) at 31V, focusing potential (FP) at 340V and entrance potential (EP) at 6.5V. Data acquisition and processing were accomplished using the Applied Biosystems Analyst version 1.6 software. The calibration curves were constructed by plotting the ratio of the peak areas of TC-G 1008 to internal standard versus TC-G 1008 concentrations and generated by weighted (1/x) linear regression analysis. The validated quantitation ranges for this method were from 1 to 2000 ng/mL for serum and 3-1500 ng/g for brain tissue with accuracy from 89.88–110.13% and from 86.54–109.51% for serum and brain tissue, respectively. The assays were reproducible with low intra- and inter-day variation (coefficient of variation less than 15%). No significant matrix effect was observed and there were no stability related problems during the routine analysis of samples.

Determination of total zinc concentration by ICP-OES

Serum samples of Swiss Albino mice or C57BL/6/Tar x CBA/Tar mice were defrosted. 200 µL of serum was transferred to digestion vessels (DigiTUBE SCP SCIENCE 50mL class A) and mixed with 1.5 mL of 65% Suprapur® nitric acid (Merck) and 5.0 mL of deionized water. Then vessels were placed in heating blocks (DigiPREP SCP SCIENCE) and were digested for 60 minutes at 120℃. After digestion vessels with solution were left to reach RT and filled with deionized water to 10 mL. The analysis was performed using PlasmaQuant PQ 9000 Analytik Jena AG. The following operating conditions of ICP-OES were used: power 13000 W, plasma gas 14.0 L/min, auxiliary gas 0.50 L/min, nebulizer gas 0.60 L/min, monitoring direction of the plasma flame was axial. Standard solution for calibration curves of zinc at the concentration of 200 µg/L was prepared by diluting zinc 1000 mg/L standard (PlasmaCAL SCP SCIENCE) with 0.5% nitric acid in deionized water. Analysis line used for zinc quantification was 206.2 nm.

Determination of total zinc concentration by LA-ICP-MS

12 µm hippocampal coronal sections from C57BL/6/Tar x CBA/Tar mice were thawed and dried at RT in the desiccator and placed in the ablation chamber. The sections were analyzed using a laser ablation (LA) system (LSX-500, CETAC Technologies, Omaha, NE, USA) with a quadrupole inductively coupled plasma mass spectrometer (ICP-MS, Elan DRC II, PerkinElmer SCIEX, Toronto, ON, Canada). The instruments were optimized daily with the use of a certified reference material of NIST SRM 610 glass, which included the nebulizer gas flow, ion lens voltage, and power of the plasma generator, and were tuned until reaching the maximal intensity for 24Mg+, 115In+, 238U+, and the oxide ratios of 232Th16O+/232Th+ < 0.2%, as well as doubly charged ions 42Ca2+/42Ca+ < 0.2%. The following isotopes were monitored in all measurements: ^{13}C, ^{66}Zn. The laser parameters were optimized to completely ablate the thin sections and to obtain measurable signals for the analyzed elements, which

required the optimization of the following laser parameters: laser energy, laser spot size, frequency of laser shots, and sample scan rate. The instrumental parameters of LA-ICP-MS were as follows: laser energy 2.7 mJ, spot size 100 µm, ablation frequency 2 Hz, scan rate 100 µm/s, nebulizer gas flow 0.9 L/min, plasma power 1250 W, pulse counting mode, dwell time 100 ms per isotope, measured isotopes ^{13}C and ^{66}Zn. The laser beam scanned a rectangular area of the sample line by line and always from left to right. The number and width of the ablation lines were set individually for each analyzed sample, with 18 lines on average. The detector recorded a time-resolved signal that was used to create a two-dimensional matrix of data points for each sample. For the statistical evaluation of the measurement data, the region of interest (ROI) containing the hippocampus was marked on maps of the distribution of elements in thin sections of brain. The ROIs were selected by drawing the shape in the imaging software tool based on the photograph of the sample taken prior to the ablation. The signals contained in the ROI were averaged and evaluated statistically.

Determination of intracellular free zinc concentration by Zinpyr-1 staining

12 µm hippocampal coronal sections from Swiss Albino mice or C57BL/6/Tar x CBA/Tar mice were incubated with 4% paraformaldehyde solution with 4% sucrose in phosphate-buffered saline (PBS) at RT for 15 min and were rinsed with 0.01 M PBS solution. The sections were then incubated with a solution of a cell-membrane permeable fluorescent probe for zinc, ZP-1 (Santa Cruz Biotechnology, sc-213182) at the concentration of 5 µM for 1h at RT. The sections were double stained with 4',6-Diamidino-2-Phenylindole, Dihydrochloride (DAPI) (Sigma Aldrich, D9542) at the concentration of 300 nM. Adjacent sections from the same mouse brains were treated with membrane-permeable zinc chelator N,N,N',N'-Tetrakis(2-pyridylmethyl)ethylenediamine (TPEN) (Santa Cruz Biotechnology, sc-200131), at the concentration of 10 µM, for 40 min, before staining with ZP-1 and DAPI

(Grabrucker et al. 2011). The sections were imaged using Leica DM6000 B microscope. The images of all compared sections were taken with the same exposure time. The images of sections incubated with TPEN before staining with ZP-1 were taken with the same exposure time as images of sections stained with ZP-1. The low-magnification, grayscale images were analyzed for the mean ZP-1 intensities using Image J. The following regions of the hippocampus were chosen for the analysis: dentate gyrus (DG), CA1 and CA3 regions.

Western blot analysis

Hippocampi of Swiss Albino mice or C57BL/6/Tar x CBA/Tar mice were homogenized in 2% sodium dodecyl-sulfate solution (SDS) (BioShop Canada Inc), denatured at 95°C for 10 min and centrifuged at 10.000 RPM at 4°C for 5 min. The total protein concentration was quantified in the supernatant using a Pierce BCA Protein Assay Kit (Thermo Fisher Scientific, Pierce Biotechnology, Rockford, IL, USA). The samples containing 10 µg of protein were prepared using Novex® Tris-Glycine SDS Sample Buffer (Thermo Fisher Scientific, Carlsbad, CA, USA) and were resolved on a 4-15 % Mini-Protean TGX Precast gels (BIO-RAD Laboratories, Inc., USA). The molecular weight marker: Spectra Multicolor Broad Range Protein Ladder (Thermo Fisher Scientific Baltic, Vilnius, Lithuania) was used. The proteins were transferred on a nitrocellulose membrane (BIO-RAD Laboratories, Inc., USA). The membranes were blocked for 60 min with 1% blocking reagent from the BM Chemiluminescence WB kit (Mouse/Rabbit) (Roche Diagnostic, Mannheim, Germany). The membranes were then incubated with mouse monoclonal antibody targeting phosphorylated CREB at Ser 133 (anti-phospho-CREB (Ser133) antibody, clone 10E9, Millipore Cat# 05-667, RRID:AB_309889, at a concentration of 0.5 µg/ml) or rabbit monoclonal antibody targeting CREB (anti-CREB antibody, Abcam Cat#ab32515, RRID:AB_2292301, at a dilution of 1:1000) or rabbit polyclonal antibody targeting BDNF (anti-BDNF antibody, Novus Cat#

NB100-98682, RRID:AB_1290643, at a dilution of 1:1000), or rabbit polyclonal antibody targeting tyrosine-phosphorylated TrkB (anti-Trk B phosphorylated (pTyr 816) antibody, Novus Cat# NBP1-03499, RRID:AB_1522601, at a concentration of 10 µg/ml), or rabbit monoclonal antibody targeting TrkB (anti-TrkB antibody, Abcam Cat#ab187041, RRID: AB_2892613, at a dilution of 1:5000), rabbit polyclonal antibody targeting metal regulatory transcription factor 1 (MTF1) (Novus Cat# NBP1-86379, RRID:AB_11033871, at a concentration of 0.2 ug/ml) or β-actin (β-actin antibody, mouse monoclonal clone AC-15, purified from hybridoma cell culture**,** Sigma-Aldrich Cat# A1978, RRID:AB_476692, at a concentration of 0.5 µg/ml**)** at 2-8°C overnight. The dilutions of primary antibodies were prepared using 0.5% blocking solution from the BM Chemiluminescence WB kit (Mouse/Rabbit). They were stored at 2-8°C and were reused up to two times. On the next day, after washing with TBST 3 x 10 min, the membranes were incubated for 30 min with horseradish peroxidase-linked (HRP-linked) secondary antibody from the BM Chemiluminescence WB kit (Mouse/Rabbit), or the anti-mouse IgG, HRP-linked, Cell Signaling Cat# 7076, RRID:AB_330924, at the dilution of 1:1000 (in case of β-actin) under constant shaking at room temperature (RT). The dilutions of secondary antibodies were always prepared fresh. After incubation with secondary antibodies, the membranes were washed with TBST 3 x 10 min. Secondary antibodies were detected using a BM Chemiluminescence WB kit (Mouse/Rabbit). The protein bands were visualized with the Fuji-LAS 4000 System. The density of each protein band was analyzed using imaging software (Fuji Image Gauge v 4.0) and was normalized by the optical density of the corresponding β-actin band.

Data and statistical analysis

Data were analyzed using GraphPad Prism v. 5.03 (GraphPad Software, San Diego, CA, USA) or STATISTICA v. 13.3 (TIBCO Software Inc, Palo Alto, CA, USA). Acute seizure tests and grip-strength tests in Swiss Albino mice or C57BL/6/Tar x CBA/Tar mice were analyzed

using unpaired Student's *t*-test or one-way analysis of variance (ANOVA) and the Dunnett's multiple comparison test. Kindling in Swiss mice was analyzed by the two-way ANOVA and the Dunnett's multiple comparison test. Kindling in C57BL/6/Tar x CBA/Tar mice was analyzed by the three-way ANOVA and the Bonferroni's multiple comparison test. The Fisher's exact probability test (https://www.graphpad.com/quickcalcs/contingency2) or the Chi-square test were employed to analyze the chimney test. Data obtained in zebrafish larvae were analyzed by the two-way ANOVA and the Bonferroni's multiple comparison test. For Western blot, ZP-1 staining, ICP-OES or LA-ICP-MS each sample was run in at least triplicate. For Western blot each sample was run in at least duplicate. These experiments were analyzed by the two-way ANOVA and the Bonferroni's multiple comparison test. All results are presented as the mean ± SEM. $p<0.05$ was considered statistically significant with 95% confidence. No statistical method was used to predetermine sample size. The exact sample size in each behavioral, EEG or biochemical experiment is shown in Supplementary file. Data were screened for outliers using the Grubbs's test (https://www.graphpad.com/quickcalcs/Grubbs1.cfm). The outliers were removed from the analyses. Data were analyzed for normality of residual errors using skewness and kurtosis. The degree of departure from normality was not significant, thus allowing the use of general linear model.

Results

TC-G 1008 is brain penetrant

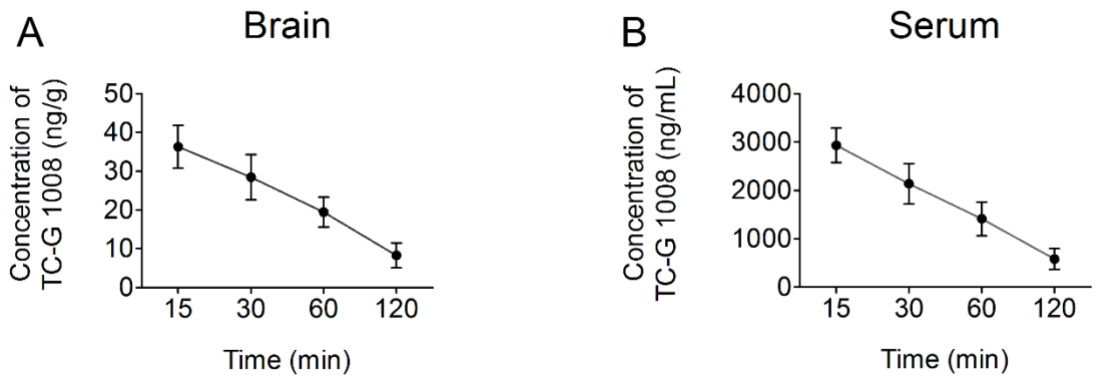

Fig 1. The concentrations of TC-G 1008 in the brain (**A**) and serum (**B**) of Swiss Albino mice over time following *i.p.* administration of a single dose of TC-G 1008 (20 mg/kg). N=4 mice per each timepoint.

First, we measured the concentration versus time profiles of TC-G 1008 in the brain and serum of Swiss Albino mice following *i.p.* administration of a single dose of TC-G 1008 (20 mg/kg) (Fig 1). The mean concentration of TC-G 1008 in the brain was 36.32 ng/g 15 min after its *i.p.* administration at a dose of 20 mg/kg and 28.48 ng/g 30 min after dosing (Fig 1A). The molecular weight of TC-G 1008 is 481.9 Da. The estimated EC_{50} values are 0.4 and 0.8 nM for rat and human receptors, respectively (Peukert et al. 2014), which corresponds to 0.193 ng/mL and 0.385 ng/mL. These data show that the concentrations of TC-G 1008 attained in the brain after its *i.p.* administration at the dose of 20 mg/kg are sufficient to occupy the GPR39 receptor. The mean concentrations of TC-G 1008 in serum were 2930 ng/mL and 2135 ng/mL after 15 and 30 min, respectively (Fig 1B). The serum levels of the studied compound were close to those obtained following oral administration of TC-G 1008 to male C57/Bl6 mice (Peukert et al. 2014). For example, the dose-normalized concentration at 60 min was 0.071 in this study and 0.06 when the compound was given orally at the dose of 10 mg/kg (Peukert et al. 2014). These data indicate that bioavailability of TC-G 1008 is comparable after both routes of administration.

The pharmacokinetic parameters of TC-G 1008 following administration of the dose of 20 mg/kg *i.p.* in Swiss Albino mice estimated using the non-compartmental approach are depicted in Table S1. TC-G 1008 was relatively slowly eliminated from serum and brain as the terminal half-life was about 50 min and the mean residence time values were over 70 min. The volume of distribution was high and significantly exceeded mouse whole body water, thus showing an extensive distribution of the studied compound to organs and tissues. However, the penetration to brain tissue was rather limited as the brain-to-serum AUC ratio was 0.014. Nevertheless, the TC-G 1008 concentrations in this organ were sufficient to exert pharmacological effects at GPR39, which prompted us to examine its behavioral effects.

TC-G 1008 and $ZnCl_2$ exert divergent effects in the MEST and 6-Hz seizure threshold tests

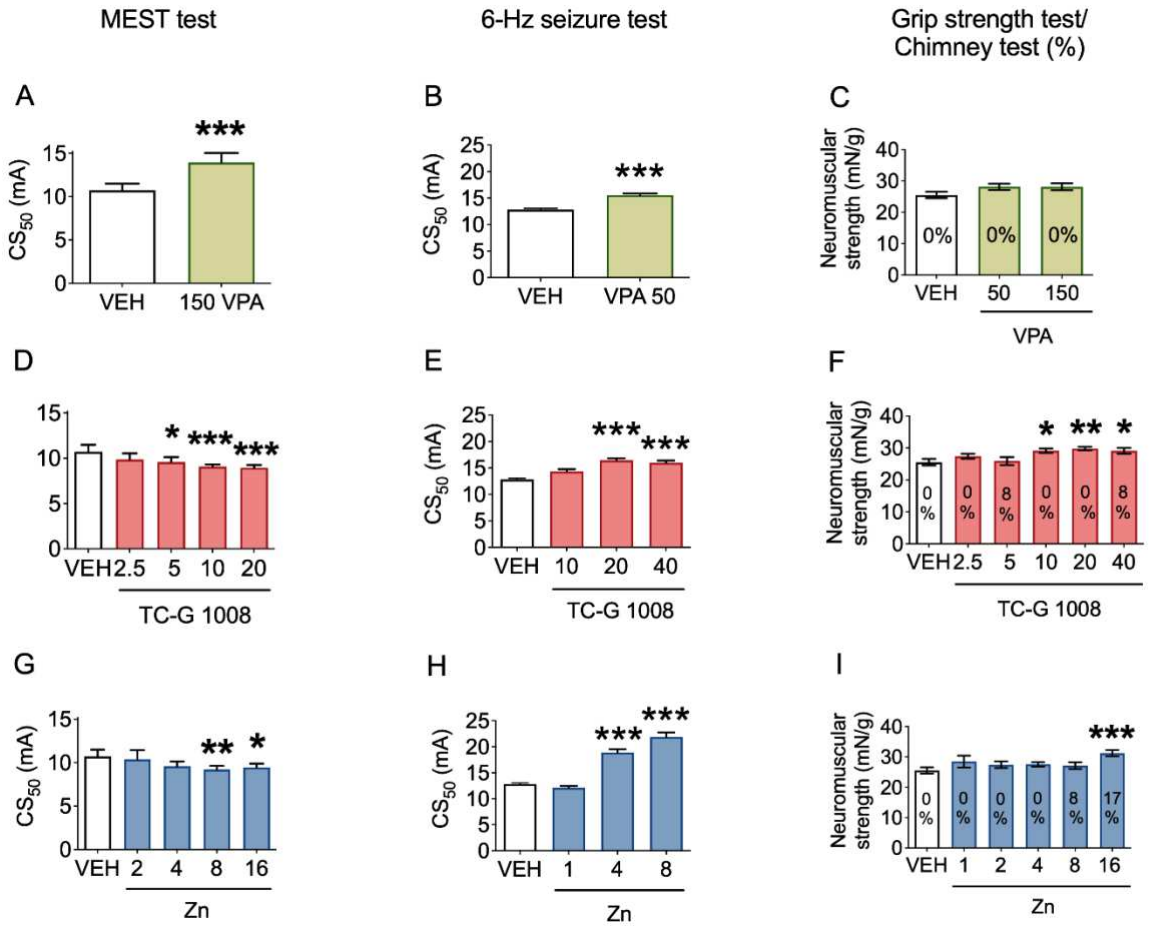

Fig 2. The effects of *i.p.* administration of single doses of VPA (**A, B, C**), TC-G 1008 (**D, E, F**) or $ZnCl_2$ (**G, H, I**) on the seizure threshold in the maximal electroshock seizure threshold (MEST) test (**A, D, G**), on the seizure threshold in the 6-Hz seizure threshold test (**B, E, H**), on neuromuscular strength in the grip-strength test and on motor coordination in the chimney test (**C, F, I**). Swiss Albino mice received VPA, TC-G 1008 or $ZnCl_2$ (the doses of compounds are shown on abscissas). Control animals received vehicle (VEH) (1% Tween 80 in 0.9% NaCl). The tests were performed 30 minutes after administration of the compounds or VEH. Data from the MEST and 6-seizure threshold test were analyzed by the Student's t-test or one-way ANOVA and the Dunnett's multiple comparison test. They are presented as CS_{50} (in mA) values with upper 95% confidence limits. Data from the grip-strength test (expressed as means ± SEM of the neuromuscular strength) and the chimney test (expressed as % of animals which displayed impairment of motor coordination in this test) were analyzed by the one-way ANOVA and Dunnett's multiple comparison test or the Chi-square test, respectively. *P<0.05, **p<0.01, *** p<0.001 (by Student's t-test or Dunnett's multiple comparison test).

TC-G 1008 and $ZnCl_2$, unlike VPA, decrease seizure threshold in the MEST test

Our first aim was to assess the impact of GPR39 receptor activation on behavioral or EEG seizures. We examined the effects of single doses of GPR39 agonists: TC-G 1008 and $ZnCl_2$, in comparison to a standard anti-seizure drug, VPA on the seizure threshold in two acute seizure-threshold tests in mice: MEST and 6-Hz-seizure threshold tests (Fig 2). Because anti-seizure drugs may impact motor coordination and neuromuscular strength, we assessed the effects of the compounds in the chimney test and the grip strength test, respectively. As TC-G 1008 was detectable in the brain tissue 30 min after its *i.p.* administration in Swiss Albino mice at a concentration sufficient to occupy the GPR39 receptor (Fig 1A), the tests examining the effects of the compounds on behavioral seizures were performed 30 min after their administration. A standard anti-seizure drug, VPA (150 mg/kg) significantly increased the threshold for tonic hindlimb extension in the MEST test (Fig 2A). In contrast, TC-G 1008 at doses of 5, 10 and 20 mg/kg (Fig 2D) and $ZnCl_2$ at doses of 8 and 16 mg Zn/kg (Fig 2G) significantly decreased the threshold for seizures in this test.

TC-G 1008 and $ZnCl_2$, as VPA, increase seizure threshold in the 6-Hz seizure threshold test

However, all three compounds, *i.e.*, VPA (50 mg/kg) (Fig 2B), TC-G 1008 at doses of 20 and 40 mg/kg (Fig 2E) as well as $ZnCl_2$ at doses of 4 and 8 mg Zn/kg (Fig 2H) significantly increased the threshold for seizures induced by 6-Hz, thus revealing divergent effects of the GPR39 agonists in the MEST and 6-Hz seizure threshold tests.

None of the examined compounds administered as a single dose significantly impaired motor coordination of mice in the chimney test (Fig 2C, 2F, 2I). In addition, single doses of VPA had no effects on the neuromuscular strength in the grip-strength test, (Fig 2C), while TC-G 1008 administered at single doses of 10, 20 and 40 mg/kg significantly increased the

neuromuscular strength of mice (Fig 2F). Similarly, a single dose of $ZnCl_2$ (16 mg Zn/kg) increased the neuromuscular strength of mice in this test (Fig 2I).

$ZnCl_2$ increases maximal seizure severity and the incidence of SE in response to kainic acid

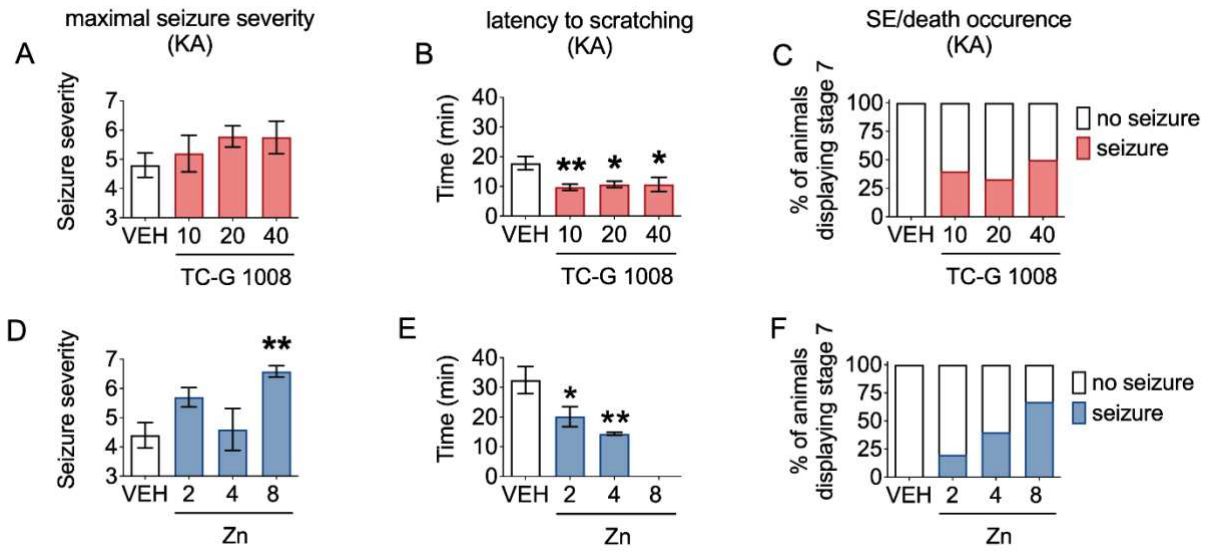

Fig 3. The effects of TC-G 1008 or $ZnCl_2$ on seizures induced by *i.p.* administration of kainic acid (KA) in Swiss Albino mice. TC-G 1008 (**A, B, C**) or $ZnCl_2$ (**D, E, F**) (the doses shown on abscissas) were administered *i.p.*, 30 min before KA (40 mg/kg, *i.p.*) treatment in Swiss Albino mice. Control animals received vehicle (VEH) (1% Tween 80 in 0.9 % NaCl). Immediately after KA administration the mice were subjected to evaluation of behavioral seizures, which lasted 2 h. Data were analyzed by the one-way ANOVA and Dunnett's multiple comparison test and are expressed as mean ± SEM or the Chi-square test. **P<0.01, *p<0.05 (the Dunnett's multiple comparison test).

Because GPR39 KO mice were previously characterized by increased susceptibility to acute seizures induced by KA (Gilad et al. 2015; Khan 2016), we next examined the effects of single doses of GPR39 agonists on acute KA-induced seizures in mice (Fig 5). $ZnCl_2$ at a dose of 8 mg Zn/kg significantly increased the maximal seizure score in response to KA (40 mg/kg) (Fig 5D). Moreover, TC-G 1008 at doses of 10, 20 and 40 mg/kg (Fig 5B) and $ZnCl_2$ at doses of 2 and 4 mg Zn/kg (Fig 5E) significantly decreased the latency to scratching. This parameter was not possible to measure after administration of the dose of 8 mg Zn/kg because mice

proceeded immediately to advanced seizure stages. The incidence of SE/ death (stage 7 seizure) was 40%, 33% and 50% after administration of TC-G 1008 at doses of 10, 20 and 40 mg/kg and KA (40 mg/kg), respectively (Chi-square test, $p>0.05$) (Fig 5C). In the case of $ZnCl_2$, the incidence of SE/ death was 20%, 40% and 67% following 2, 4 and 8 mg Zn/kg and KA (40 mg/kg), respectively (Chi-square test, $p<0.05$) (Fig 5F). Thus, $ZnCl_2$ significantly increased the incidence of SE/ death in response to KA. None of control mice injected with KA (40 mg/kg) exhibited SE/death.

TC-G 1008 increases the mean duration of epileptiform-like events in zebrafish larvae

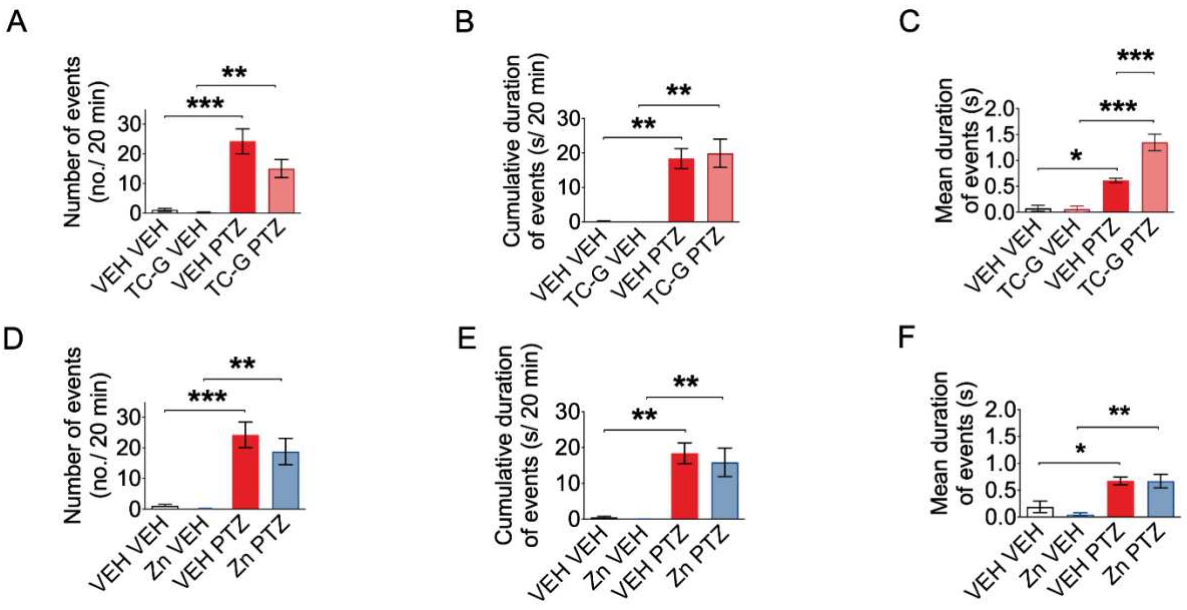

Fig 4. Electrophysiological recordings from the optic tectum of zebrafish larvae exposed to TC-G 1008 or $ZnCl_2$ and PTZ. Zebrafish larvae were incubated with VEH, TC-G 1008 (70 µM) or $ZnCl_2$ (65 µM) for 20 h, and subsequently exposed to VEH or PTZ (20 mM) for 5 min. In experiments in zebrafish embryo medium constituted VEH. The EEG recordings began 5 min after the removal of larva from VEH/PTZ solution and lasted 20 min. Results are expressed as means ± SEM of the number of epileptiform-like events, the cumulative duration of epileptiform-like events, and the mean duration of epileptiform-like events during 20 min of recordings. Data were analyzed using a two-way ANOVA and the Bonferroni's multiple comparison test. *P<0.05, **p<0.01, ***p<0.001 (by the Bonferroni's multiple comparison test).

To characterize the EEG effects of GPR39 agonists on seizures, we performed PTZ-induced acute seizure model in zebrafish larvae (Fig 6A-F). Exposure to PTZ (20 mM) significantly increased the number of epileptiform-like events, the cumulative duration of epileptiform-like events and the mean duration of epileptiform-like events in zebrafish larvae. TC-G 1008 (70 µM) increased the mean duration of epileptiform-like events in larvae exposed to PTZ, compared to VEH (Fig 6C), but it did not affect the number of events (Fig 6A) or the cumulative duration of events (Fig 6B). Administration of $ZnCl_2$ (65 µM) in larvae exposed to PTZ did not affect the mean duration of epileptiform-like events (Fig 6D), the number of events (Fig 6E) or the cumulative duration of events (Fig 6F), compared to VEH. Administration of TC-G 1008 (70 µM) or $ZnCl_2$ (65 µM) also did not affect the examined parameters in larvae treated with VEH instead of PTZ (Fig 6A-F).

TC-G 1008 facilitates the development of PTZ-induced epileptogenesis in mice

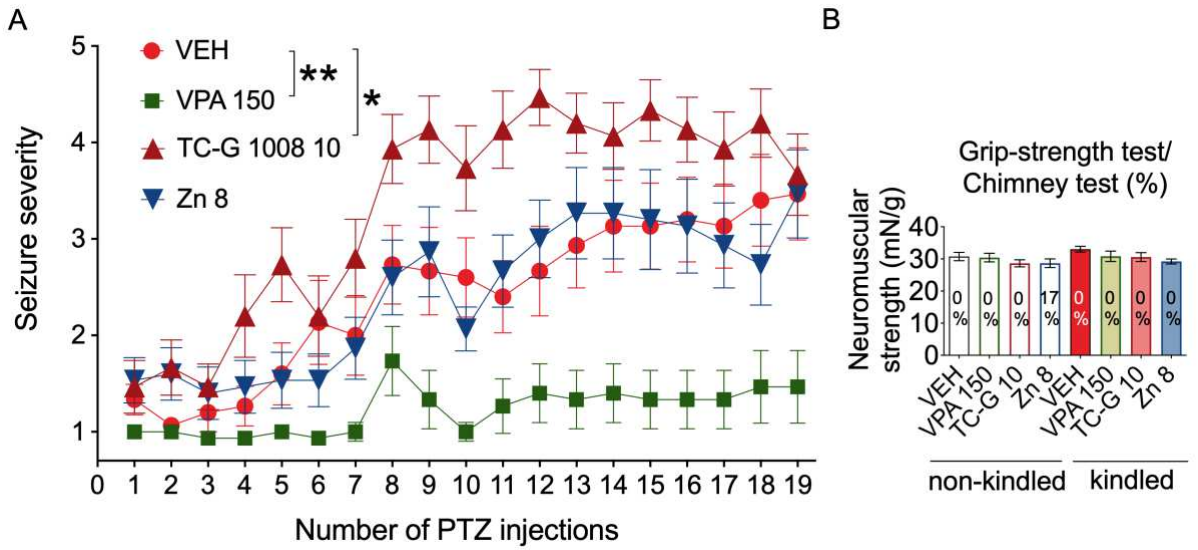

Fig 5. (**A**) The effects of chronic treatment with VPA, TC-G 1008 or $ZnCl_2$ on the development of PTZ kindling in Swiss Albino mice. VPA (150 mg/kg), TC-G 1008 (10 mg/kg), $ZnCl_2$ (8 mg Zn/kg) or VEH (1% Tween 80 in 0.9% NaCl) were injected *i.p.* once daily on every alternate day during weekdays. 30 min later, PTZ (40 mg/kg) was injected *i.p.* Immediately after each PTZ injection the mice were subjected to evaluation of behavioral seizures, which lasted 30 min. The total number of PTZ injections was 19. Data are expressed as means ± SEM of seizure severity and were analyzed by repeated measures ANOVA and a Dunnett's multiple comparison test. *P<0.05,

p<0.01 (by the Dunnett's multiple comparison test) (B**) The effects of chronic treatment with VPA, TC-G 1008 or $ZnCl_2$ and PTZ kindling on neuromuscular strength in the grip-strength test and motor coordination in the chimney test in Swiss Albino mice. The non-kindled mice received the respective doses of drugs: VPA (150 mg/kg), TC-G 1008 (10 mg/kg), $ZnCl_2$ (8 mg Zn/kg) or VEH (1% Tween 80 in 0.9% NaCl) but received saline (0.9% NaCl) instead of PTZ. The neuromuscular strength and motor coordination were assessed in kindled and non-kindled mice on the last day of PTZ kindling. Data from the grip-strength test (expressed as means ± SEM of the neuromuscular strength) and chimney test (expressed as % of animals which displayed impairment of motor coordination in this test) were analyzed by the two-way ANOVA or the Fisher's exact test, respectively

To examine the chronic effects of GPR39 agonists on epileptogenesis, we utilized PTZ-induced kindling model of epilepsy in mice. In this model, PTZ gradually increased the seizure severity over time. VPA decreased the maximal seizure severity compared to VEH ($p=0.001964$, Dunnett's multiple comparison test). In contrast, TC-G 1008 (10 mg/kg) increased the maximal seizure severity compared to VEH ($p=0.024368$, Dunnett's multiple comparison test), while $ZnCl_2$ did not significantly affect this parameter. After 19 injections of PTZ (40 mg/kg), the percentage of fully kindled Swiss albino mice was 6.7% of mice treated with VPA (150 mg/kg), 53% of mice treated with VEH, 67% of mice treated with $ZnCl_2$ (8 mg Zn/kg) and 87% of mice treated with TC-G 1008 (10 mg/kg) (Fisher's exact test $p=0.0142$ in the case of VPA 150, $p=0.7104$ in the case Zn 8, $p=0.0352$ in the case TC-G 1008 10). Thus, TC-G 1008 significantly increased the percentage of fully kindled mice in this model. To reduce possible mortality in mice treated with TC-G 1008 (10 mg/kg), exhibiting consecutive stage 5 seizures, kindling was terminated after 19 injections of PTZ (40 mg/kg) (Fig 5A).

We also assessed the neuromuscular strength and motor coordination of non-kindled and kindled mice that received the examined drugs in a repeated manner. After 19 injections, none of the drugs significantly affected the neuromuscular strength or motor coordination in non-kindled mice. Similarly, after 19 injections, none of the compounds significantly affected the outcomes of these tests in mice kindled with PTZ (40 mg/kg) (Fig 5B).

GPR39 KO mice do not differ from WT mice in terms of the seizure threshold in the MEST test

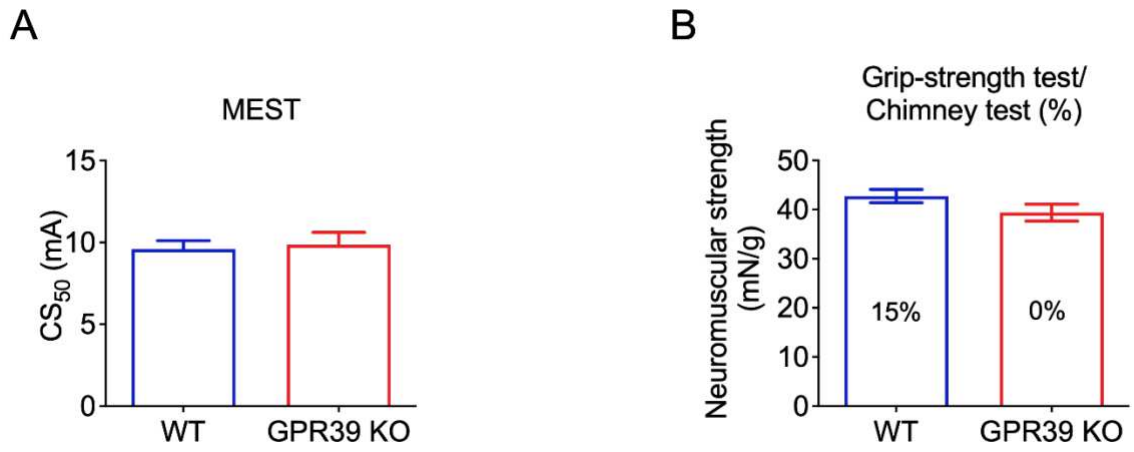

Fig 6. The effects of GPR39 KO in C57BL/6/Tar x CBA/Tar mice on the seizure threshold in the MEST test (**A**), on neuromuscular strength in the grip-strength test and on motor coordination in the chimney test (**B**). (**A**) Data are expressed as CS_{50} (in mA) with upper 95% confidence limits and were analyzed by the Student's t-test. (**B**) Neuromuscular strength (in the Grip-strength test) and motor coordination (in the chimney test) were assessed in experimentally naïve GPR39 KO and WT mice. Data from the grip-strength test (expressed as means ± SEM of the neuromuscular strength) and chimney test (expressed as % of animals which displayed impairment of motor coordination in this test) were analyzed by the Student's t-test or the Fisher's exact test, respectively.

Our second aim was to explore the role of GPR39 gene in acute seizures and epileptogenesis. We generated GPR39 KO mice model in mixed genetic background. GPR39 KO and WT C57BL/6/Tar x CBA/Tar mice were subjected to the MEST test. The seizure threshold did not differ between the GPR39 KO and WT mice in this test (Fig 6A). Also, the neuromuscular strength or motor coordination did not differ significantly between GPR39 KO and WT mice (Fig 6B).

TC-G 1008 facilitates the development of PTZ-induced epileptogenesis in WT but not in GPR39 KO mice

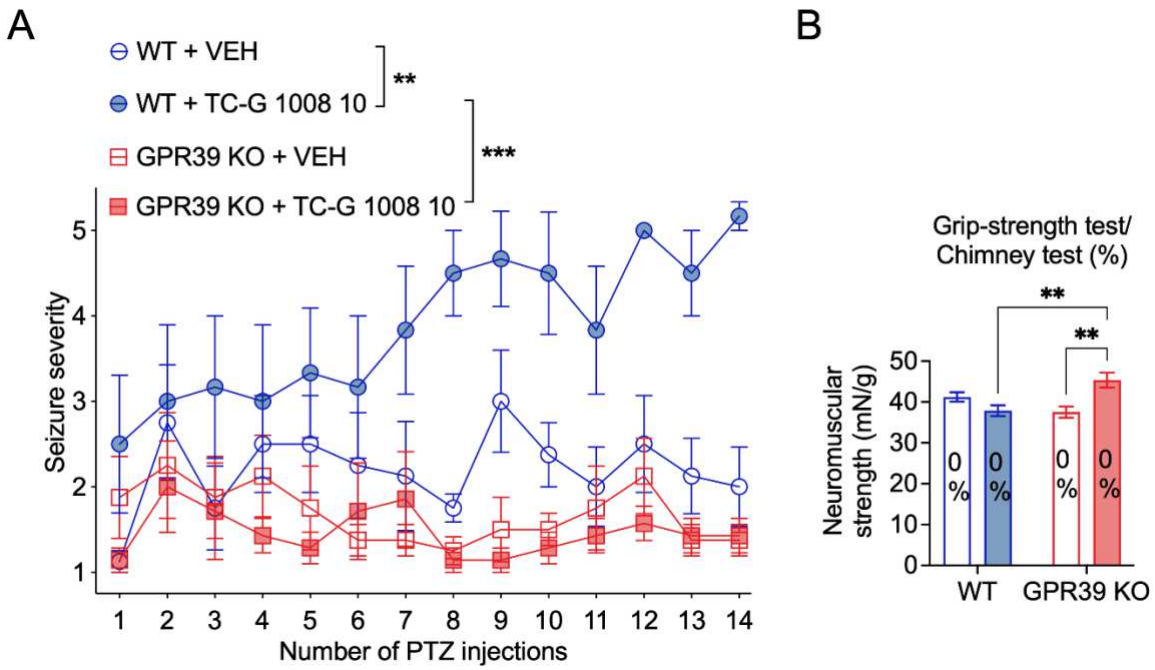

Fig 7. (**A**) The effects of GPR39 KO and chronic treatment with TC-G 1008 on the development of PTZ kindling in C57BL/6/Tar x CBA/Tar mice During PTZ kindling, WT and GPR39 KO mice were injected *i.p.* once daily with TC-G 1008 (10 mg/kg) or VEH (1% Tween 80 in 0.9 % NaCl) on every alternate day during weekdays. 30 min later, the mice were injected *i.p.* with PTZ (25 mg/kg). Immediately after each PTZ injection the mice were subjected to evaluation of behavioral seizures, which lasted 30 min. The total number of PTZ injections was 14. Data are expressed as means ± SEM of seizure severity and were analyzed by the three-way repeated measures ANOVA and the Bonferroni's multiple comparison test. ***P<0.001, **P<0.01 (the Bonferroni's multiple comparison test). The effects of PTZ kindling in GPR39 KO or WT (C57BL/6/Tar x CBA/Tar) mice and chronic treatment with TC-G 1008 or VEH on neuromuscular strength in the grip-strength test and motor coordination in the chimney test (**B**) Neuromuscular strength and motor coordination were assessed on the last day of PTZ kindling in GPR39 KO or WT mice treated with TC-G 1008 (10 mg/kg) or VEH. Data from the grip-strength test (expressed as means ± SEM of the neuromuscular strength) were analyzed by the two-way ANOVA and the Bonferroni's multiple comparison test. Data from the chimney test are expressed as % of animals which displayed impairment of motor coordination in this test. **p<0.01 (the Bonferroni's multiple comparison test).

To examine the role of GPR39 gene in epileptogenesis, GPR39 KO and WT C57BL/6/Tar x CBA/Tar mice were subjected to chronic, PTZ-induced kindling model of epilepsy. The maximal seizure severity did not differ between the GPR39 KO and WT mice subjected to this model. However, chronic administration of TC-G 1008 increased the maximal

seizure score in WT mice. Such effect was not observed in GPR39 KO mice (Fig 7A). These data show that TC-G 1008 facilitated the development of PTZ-epileptogenesis by acting at the GPR39 receptor. After 14 injections of PTZ (25 mg/kg), the percentage of fully kindled mice was 25% in the case of WT VEH group, 83.3% in the case of WT TC-G 1008 10 group, 0% in the case of KO VEH and 0% in the case of KO TC-G 1008 group. The Fisher's exact test p=0.0210 regarding WT TC-G 1008 group showed that TC-G 1008 significantly increased the percentage of fully kindled WT mice in this model. Furthermore, the percentage of fully kindled WT (C57BL/6/Tar x CBA/Tar) mice that were administered with TC-G 1008 was similar (>80%) to Swiss Albino mice subjected to treatment with this compound at the end of both kindling procedures. To reduce possible mortality in C57BL/6/Tar x CBA/Tar mice treated with TC-G 1008 (10 mg/kg), exhibiting consecutive stage 5 seizures, kindling was terminated after 14 injections of PTZ (25 mg/kg). Surprisingly, 14 injections of TC-G 1008 increased the neuromuscular strength in GPR39 KO mice subjected to kindling induced by PTZ (25 mg/kg), but not in WT mice that underwent this procedure (Fig 7B).

GPR39 KO mice subjected to the PTZ-kindling model display decreased total serum zinc concentration but no significant alterations in total zinc in the hippocampus

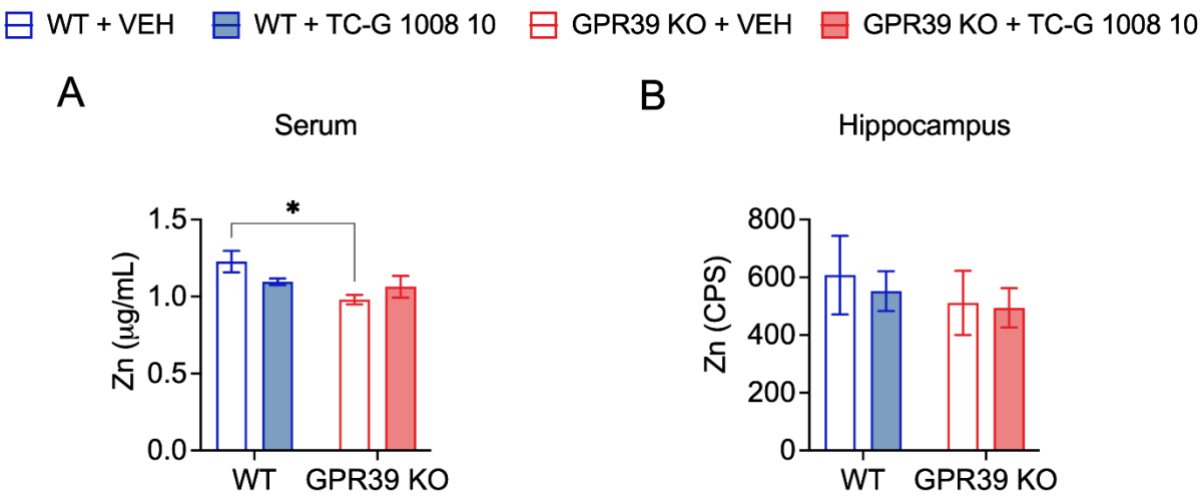

Fig 8. The effects of PTZ kindling in GPR39 KO or WT (C57BL/6/Tar x CBA/Tar) mice and chronic treatment with TC-G 1008 (10 mg/kg) or VEH on total zinc in serum **(A)** and total zinc in the hippocampus **(B)**. The PTZ kindling in GPR39 KO or WT (C57BL/6/Tar x CBA/Tar) mice consisted of 14 injections of PTZ (25 mg/kg). The biochemical analyses were performed at 24 h after the last PTZ injection. **(A)** Total zinc was measured in serum by ICP-OES. **(B)** Total zinc was analyzed semi-quantitatively in coronal hippocampal sections by LA-ICP-MS. Results are presented as counts per second (CPS). Data were analyzed by the two-way ANOVA and the Bonferroni's multiple comparison test. *P<0.05 (by the Bonferroni's multiple comparison test).

Our next aim was to provide more insight into the relationship between the function of the GPR39 receptor and different pools of zinc (total zinc and $[Zn^{2+}]_I$) in the context of epileptogensis. We analyzed total zinc concentration in sera and hippocampi of GPR39 KO and WT C57BL/6/Tar x CBA/Tar mice subjected to the PTZ-kindling model. At 24 h after the completion of the kindling paradigm, total serum zinc concentration was lower in VEH-treated GPR39 KO mice subjected to the PTZ-kindling model, compared with VEH-treated WT mice that underwent this procedure. Chronic administration of TC-G 1008 did not affect total serum zinc concentration in either GPR39 KO or WT mice subjected to this paradigm (Fig 8A). Moreover, a semi-quantitative analysis by means of LA-ICP-MS method applied to hippocampal slices did not reveal statistically significant differences in total zinc in the hippocampus between GPR39 KO or WT that were treated with either VEH or TC-G 1008 during PTZ-kindling model (Fig 8B).

Chronic treatment with TC-G 1008 increases $[Zn^{2+}]_I$ in the hippocampus of WT mice subjected to the PTZ-kindling model

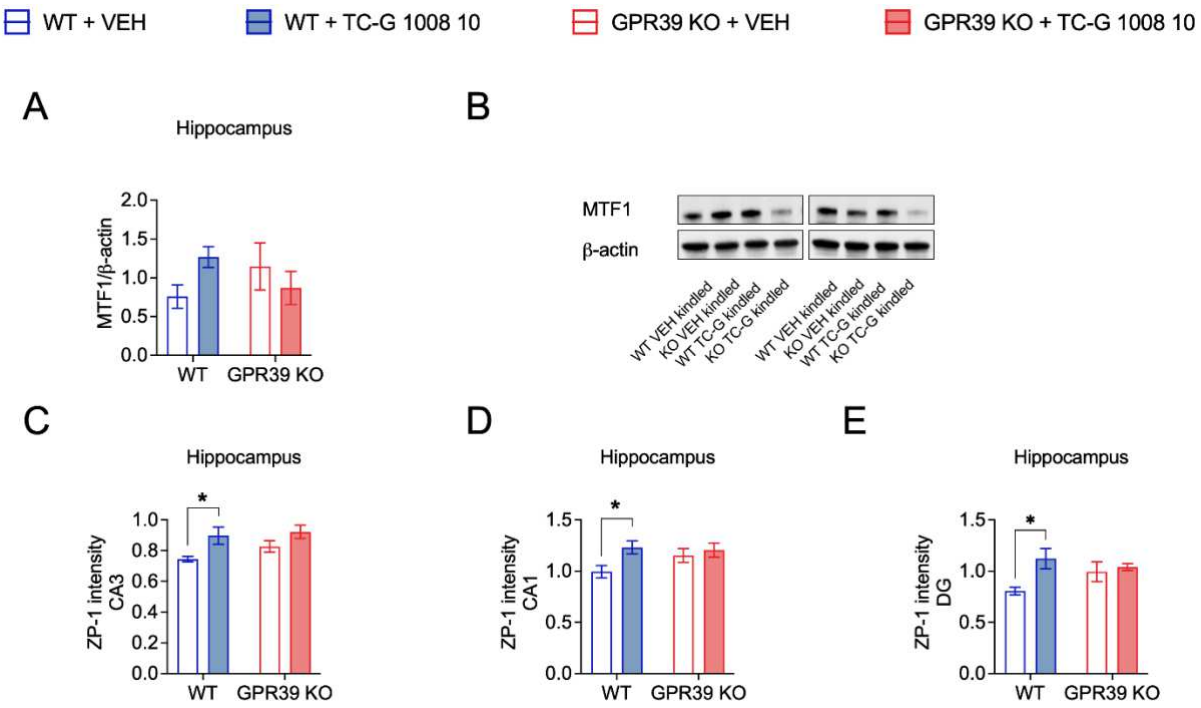

Fig 9. The effects of PTZ kindling in GPR39 KO or WT (C57BL/6/Tar x CBA/Tar) mice and chronic treatment with TC-G 1008 (10 mg/kg) or VEH on the relative expression of MTF1 protein in the hippocampus **(A)** and on $[Zn^{2+}]_I$ in the hippocampus **(C-E)**. The PTZ kindling in GPR39 KO or WT (C57BL/6/Tar x CBA/Tar) mice consisted of 14 injections of PTZ (25 mg/kg). The biochemical analyses were performed at 24 h after the last PTZ injection. **(A)** The results (mean ± SEM) are presented as the MTF1/β-actin ratio and were analyzed by the two-way ANOVA. (**B**) Representative blots of MTF1 in the hippocampi of mice. The observed band (~130 kDa). **(C-E)** The ratio of mean Zinpyr-1 (ZP-1) grey values between mouse sections from WT or GPR39 KO mice that received either TC-G 1008 or VEH and underwent PTZ kindling in the CA3 (**A**), CA1 (**B**) or DG (**C**) regions of the hippocampus. Data were analyzed by the two-way ANOVA and the Bonferroni's multiple comparison test. *P<0.05 (by the Bonferroni's multiple comparison test).

Furthermore, $[Zn^{2+}]_I$ intensity, analyzed by a fluorescent probe ZP-1, did not difer significanly between hippocampal sections from GPR39 KO and WT mice at 24 h after the completion of the kindling paradigm (Fig 9D-F). However, chronic treatment with TC-G 1008 increased $[Zn^{2+}]_I$ in the CA3 (Fig 9D), CA1 (Fig 9E) and DG (Fig 9F) regions of the hippocampus of WT mice subjected to this model of epilepsy. As MTF1 is a candidate $[Zn^{2+}]_I$ sensor (Carpenter and Palmer 2017), we examined its expression at the protein level in the hippocampi of those mice. At 24 h after the completion of the kindling paradigm, there were no statistically significant changes in the level of expression of MTF1 protein in the hippocampus between GPR39 KO and WT mice. Increased $[Zn^{2+}]_I$ in sections from WT mice treated with TC-G 1008 during the kindling paradigm was parallel to increased (by 86 %) expression of MTF1 protein (the result was not statistically significant).

Chronic treatment with TC-G 1008 markedly increases activation of CREB in the hippocampus of GPR39 KO mice subjected to the PTZ-kindling model

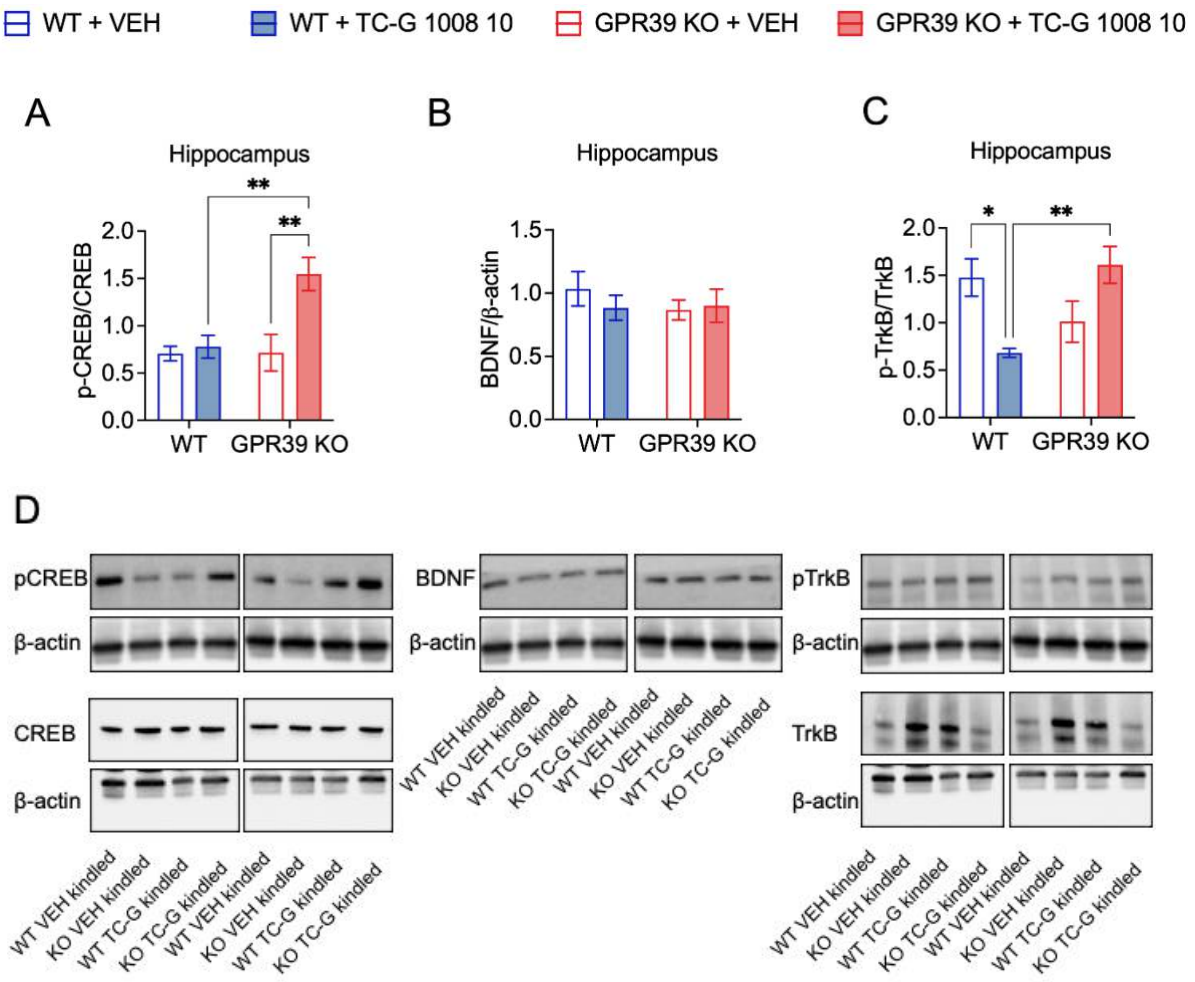

Fig 10. The effects of PTZ kindling in GPR39 KO or WT (C57BL/6/Tar x CBA/Tar) mice and chronic treatment with TC-G 1008 (10 mg/kg) or VEH on the relative expression of proteins: p-CREB, CREB, BDNF, p-TrkB or TrkB in the hippocampus. The results (mean ± SEM) are presented as the p-CREB/CREB (**A**) or BDNF/β-actin (**B**) or p-TrkB/TrkB (**C** ratio and were analyzed by the two-way ANOVA and a Bonferroni's multiple comparison test. **P<0.01 (by the Bonferroni's multiple comparison test). **(D)** Representative blots of p-CREB, CREB (~46 kDa), BDNF (~14 kDa), p-TrkB, TrkB (~140 kDa) and β-actin (~42 kDa) in the hippocampi of mice.

Finally, we examined changes in expression of proteins of TC-G 1008 signaling pathway. VEH-treated GPR39 KO and WT mice subjected to the PTZ-kindling model did not differ significantly in p-CREB/CREB, BDNF or p-TrkB/TrkB in the hippocampus at 24 h after the completion of the model (Fig 9A-C). Surprisingly, chronic administration of TC-G 1008

markedly and significantly increased the expression of p-CREB protein (by 137%) and the p-CREB/CREB ratio (by 115%) in the hippocampus of GPR39 KO mice but not in WT mice subjected to this procedure (Fig 9A). These data suggest non-selective activity of TC-G 1008 on CREB activation upon the GPR39 receptor. The p-TrkB/TrkB ratio was also increased (by 59%) in the hippocampus of GPR39 KO treated with TC-G 1008 (the result was not significant). Furthermore, chronic treatment with TC-G 1008 significantly decreased p-TrkB/TrkB ratio (by 54%) in the hippocampus of WT mice (Fig 9C).

Discussion and Conclusions:

There are two main findings coming from our study. First, TC-G 1008, small molecule agonist of the GPR39 receptor, aggravated epileptogenesis in an animal model of epilepsy by acting at GPR39. Second, this compound induced non-selective activity upon GPR39 in terms of CREB activation in the hippocampus.

As one of the first pharmacological tool compounds for GPR39, TC-G 1008 has been used extensively to characterize the function of the receptor (Laitakari et al. 2021) but no study up to date has demonstrated *in vivo* that the effects of TC-G 1008 are indeed mediated by GPR39. TC-G 1008 was initially described as selective for GPR39 (Peukert et al. 2014) but a further study suggested that it is rather a specific one as it may also bind to the serotonin 5HT1A receptor (Sato et al. 2016). Although the possibility of TC-G 1008 acting at another target was introduced, investigations that utilized this compound were directly translated to the effects of GPR39 activation and conclusions were driven on the therapeutic potential of such intervention. Our study shows that it is crucial to evince that the effects obtained with TC-G 1008 in certain experimental context are GPR39-dependent.

The compound aggravated acute PTZ-induced seizures in zebrafish, as shown with EEG assay and facilitated the development of PTZ-kindling in mice. The effects of TC-G 1008 in the chronic, PTZ-induced kindling model of epilepsy in WT C57BL/6/Tar x CBA/Tar mice were similar with those observed in Swiss Albino mice, while TC-G 1008 had no effect in GPR39 KO mice. Thus, by combining the observation on behavioral effects of TC-G 1008 in genetically unmodified mice and GPR39 KO mice we found that TC-G 1008 facilitated PTZ-induced epileptogenesis *via* GPR39 receptor. Noteworthy is the fact that we examined the effects of TC-G 1008 on behavioral seizures in mice after determining that the concentrations of TC-G 1008 attained in the brain following its *i.p.* administration are sufficient to occupy the GPR39 receptor.

We found no impact of the GPR39 gene KO on either acute seizures induced by an electrical stimulus or on epileptogenesis. However, TC-G 1008 facilitated the PTZ-epileptogenesis by acting at GPR39, thereby showing for the first time that activation of GPR39 aggravated epileptogenesis. Our data obtained with the aid of this model thus argue against GPR39 activation being a therapeutic strategy for treating epilepsy. They are in contrast to the initial hypothesis. We conjectured anti-seizure/antiepileptogenic effects of GPR39 receptor activation based on previous study in which GPR39 KO mice displayed higher susceptibility to acute seizures induced by KA (Gilad et al. 2015; Khan 2016).

The above-mentioned finding might have important therapeutic implications. Drug discovery efforts have focused on GPR39 (Bassilana et al. 2014; Fjellstrom et al. 2015; Frimurer et al. 2017; Grunddal et al. 2021). GPR39 agonism was often suggested as a novel pharmacological strategy (Laitakari et al. 2021). On the other hand, GPR39 antagonism was suggested to be beneficial in myocardial infarction (Methner et al. 2021). Enhanced expression of GPR39 was found in the aging human brain (Davis et al. 2021) and in cancers (Gutierrez-Ruiz et al. 2022). Taken together, current data show the Janus faces of the GPR39 receptor as a target for pharmacological intervention. GPR39 agonism might be beneficial in diseases, *e.g.*, depression (Mlyniec et al. 2016; Sah et al. 2021; Starowicz et al. 2019) but worsen outcome of neurological diseases/ epilepsies may be added to possible side-effects of such intervention.

In the previous study GPR39 KO mice bred on C57BL/6 genetic background displayed higher maximal seizure severity score in response to an *i.p.* injection of a single dose of KA (10 mg/kg) (Gilad et al. 2015). The GPR39 KO model used in the present study was established in mixed genetic background C57BL/6/Tar x CBA/Tar. The genetic background may account for seizure susceptibility (Schauwecker 2011). The dose of KA used in the study of Gilad et al. (2015) produced stage 5 seizures (loss of posture or status epilepticus) in 27% of the WT mice. Because we hypothesized that GPR39 agonist may protect from seizures induced by KA, we

examined the effects of TC-G 1008 and $ZnCl_2$ on seizures induced by a single dose of KA of 40 mg/kg *i.p.* This dose of KA previously produced severe seizures in all examined mice (Lee et al. 2000). $ZnCl_2$ increased the maximal seizure severity in response to KA (40 mg/kg) and both $ZnCl_2$ and TC-G 1008 decreased the latency to scratching. Thus, aggravation of acute KA-induced seizures was observed in both GPR39 KO mice (Gilad et al. 2015) and mice administered with TC-G 1008. However, in acute KA-seizure model we cannot exclude the involvement of other targets such as 5-HT1A receptor in the activity of TC-G 1008 or $ZnCl_2$.

GPR39 KO mice subjected to the PTZ-kindling model displayed decreased total serum zinc concentration, compared to WT mice that underwent this procedure. This data strengthens the link between the GPR39 receptor and zinc. The changes in serum were, however, not accompanied by changes in total zinc in the hippocampus, as examined semi-quantitatively by LA-ICP-MS. Serum $[Zn^{2+}]_I$ (measured with ZP-1) was proposed to better reflect body's zinc status than total serum zinc and it did not correlate with the total serum concentration of zinc measured by ICP-MS (Alker et al. 2019). We therefore analyzed $[Zn^{2+}]_I$ semi-quantitatively by ZP-1 in hippocampal slices.

In addition, previous studies using fluorescent, cell membrane permeable probes demonstrated the association between $[Zn^{2+}]_I$ and SE. Staining with TFL-Zn of hippocampal slices from pilocarpine-treated rats for $[Zn^{2+}]_I$ showed increased staining in the CA1 region, which appeared 1 day after SE and declined 2–4 days after (van Loo et al. 2015). Moreover, staining of hippocampal sections with TFL-Zn revealed that zinc accumulated in CA1 and CA3 neurons after KA-induced seizures (Lee et al. 2000). The increase in $[Zn^{2+}]_I$ in the hippocampus of WT mice that underwent PTZ kindling and treatment with TC-G 1008 might thus be indicative of the relationship between $[Zn^{2+}]_I$ and enhanced epileptogenesis. Furthermore, in the study of van Loo et al. 2015 the levels of MTF1 expression were increased 6 and 12 h after pilocarpine-induced SE and returned to basal values thereafter. We analyzed $[Zn^{2+}]_I$ and MTF1

at one time point (at 24 h after the last injection of PTZ) and we did not observe robust changes in either $[Zn^{2+}]_I$ or its sensor (Carpenter and Palmer 2017) in mice experiencing enhanced epileptogenesis perhaps due to the time of sample collection for the analysis.

The increase in p-CREB/CREB ratio in the hippocampus of kindled GPR39 KO mice may be induced by TC-G 1008 acting at the 5-HT1A receptor (Sato et al. 2016). Both TC-G 1008 and $ZnCl_2$ may act at this subtype of serotonin receptor. As GPR39, 5HT1A receptor belongs to GPCRs. The postsynaptic 5HT1A heteroreceptor is highly expressed in the hippocampus. Depending on the engagement of G protein subunits, 5HT1A activation may either increase cAMP level and subsequently increase phosphorylation of CREB or it may produce the opposite effects, *i.e.*, decrease cAMP and decrease CREB phosphorylation. In addition to G-proteins, 5HT1A signals via β-arrestin pathway (Salaciak and Pytka 2021). TC-G 1008 binding to 5-HT1A (Sato et al. 2016) was shown using the PRESTO-Tango GPCR-ome assay, which is based on measurement of G-protein independent β-arrestin. Furthermore, 5HT1A and GPR39 receptors may oligomerize (Mlyniec et al. 2021). Also, zinc is an allosteric modulator of 5HT1A receptor, inducing a biphasic, concentration-dependent effect, either its activation (in sub-μM concentrations) or inhibition (in sub-mM concentrations) (Satala et al. 2016). Our data implies that TC-G 1008 may bind to 5HT1A and affect CREB phosphorylation via this receptor. This finding might be important for the understanding of the literature accumulating in recent years on TC-G 1008 as a ligand of GPR39, as some of the effects may have been induced by off-target(s).

A limitation for the above conclusion is that all mice from which we obtained samples were subjected to a model of epilepsy. However, the GPR39 KO mice treated with VEH did not differ from GPR39 KO mice treated with TC-G 1008 in terms of the behavioral seizure scores in this model, which indeed suggest that TC-G 1008, and not PTZ-induced kindling itself, affected CREB activation in GPR39 KO mice.

The effects of both acute and chronic treatment with the studied compounds and models of acute seizures or chronic PTZ-kindling model of epilepsy on different pools of zinc and expression of proteins of the GPR39 signaling pathway in genetically unmodified mice are shown in Supplementary file (Fig S2-10). We chose the doses of compounds used in MES or 6-Hz seizure models based on the outcome of the respective seizure-threshold tests and we terminated PTZ kindling based on the seizure score for the group which displayed the highest seizure score, i.e., either TC-G 1008 or TC-G 1008 in WT mice group. As consequence, the doses of compounds used for biochemical analysis vary between MES and 6-Hz seizure model and the total number of PTZ injections (as well as the dose of PTZ) differ between kindling in genetically unmodified and GPR39 KO mice, thus affecting the biochemical outcomes. For instance, the lack of significant differences in $[Zn^{2+}]_I$ in PTZ-kindled Swiss Albino mice that received TC-G 1008 (Fig S7) may be explained by the dose of PTZ and the number of injections compared to those used in C57BL/6/Tar x CBA/Tar mice.

Undoubtedly, the relationship between zinc signaling and seizures/epilepsy is complex as both extracellular zinc and $[Zn^{2+}]_I$ may produce either protective or detrimental effects by interacting with a variety of targets, raising the question how changes in extracellular zinc/ $[Zn^{2+}]_I$ concentrations influence its molecular targets and which of the effects will be prevailing (Doboszewska et al. 2019). Possible mechanisms linking GPR39, $[Zn^{2+}]_I$ and seizures/epilepsy include potassium-chloride co-transporter 2 (KCC2). KCC2 maintains low intracellular chloride concentration and is indispensable for inhibitory function of $GABA_A$ receptor (Moore et al. 2017). Activation of GPR39 by extracellular zinc induced up-regulation of KCC2 (Gilad et al. 2015; Khan 2016) and inhibited the release of the main excitatory neurotransmitter glutamate (Lu and Mackie 2016). Conversely, an increased $[Zn^{2+}]_I$ inhibited KCC2 activity (Hershfinkel et al. 2009). Therefore, $[Zn^{2+}]_I$ may play a key role in mediating the balance between neuronal inhibition/ excitation.

We found that administration of TC-G 1008 at a low dose, which was ineffective in the MEST test, in mice subjected to MES seizures, was accompanied by decreased $[Zn^{2+}]_I$ in the CA1 and CA3 regions of the hippocampus (Fig S5). Moreover, administration of TC-G 1008 or $ZnCl_2$ at doses which were effective in the 6-Hz-threshold test, in mice subjected to 6-Hz seizures, was accompanied by decreased $[Zn^{2+}]_I$ in the CA1 and DG regions (Fig S6). Thus, the distinct effects of TC-G 1008 in the MEST and 6-Hz seizure threshold tests, *i.e*, either seizure threshold decreasing or increasing effects, respectively, might be associated with hippocampal $[Zn^{2+}]_I$.

CREB (Mertz et al. 2020; Wang et al. 2020), BDNF (Iughetti et al. 2018) and TrkB (Lin et al. 2020) proteins are of interest in terms of seizures/epileptogenesis. p-CREB expression increased 3 min after seizures induced by *i.p.* administration of a single dose of PTZ (55 mg/kg) in the hippocampus and cortex (Moore et al. 1996). BDNF and p-TrkB increased in animal models and humans with epilepsy in the temporal and hippocampal areas. Furthermore, the inhibition of BDNF signaling was suggested as a strategy for the treatment of epilepsy (Iughetti et al. 2018). However, we observed that the changes in protein expression did not correspond to the behavioral outcomes. For example, in the PTZ-kindling model in Swiss Albino mice TC-G 1008, $ZnCl_2$ and VPA facilitated, had no effect or suppressed epileptogenesis, respectively, but all compounds decreased the p-CREB/CREB and p-TrkB/TrkB ratios in the hippocampus of kindled mice (Fig S10).

Regarding the biochemical effects of acute or chronic administration of the studied compounds in sham/ non-kindled (control) animals we found a tendency towards activation of CREB and TrkB after acute but not chronic treatment (Fig S8-S10). In a previous study TC-G 1008 administered at a single dose increased the level of BDNF protein expression at 24 h after administration (Mlyniec et al. 2016). We did not observe changes in BDNF protein level after acute treatment with TC-G 1008, which might be due to the time of analysis (30 min after

administration in the present study *vs.* 24 h after administration in the study by Mlyniec et al. (2016). However, when TC-G 1008 was administered acutely and the hippocampal tissue was obtained for the analysis immediately after a behavioral procedure (namely, the forced swim test (FST), which is used for screening for antidepressant drugs), there was a tendency towards increased BDNF protein expression 30 min after administration (Starowicz et al. 2019). Furthermore, in the same study TC-G 1008 was administered chronically (for 14 days) and the expression of BDNF measured at 24 h after the FST did not change (Starowicz et al. 2019). Similarly, we did not observe changes in BDNF protein level after chronic administration of TC-G 1008 at 24 h after the last dose in the chronic paradigm (Fig S10 E). Hence, the activation of CREB-BDNF-TrkB pathway by TC-G 1008 may be time-dependent and transient. More importantly, the activation of components of this signaling pathway by TC-G 1008 may also result from its effect at targets other than GPR39, as shown in the present study with the aid of GPR39 KO mice.

Serum zinc level was suggested as a biomarker in epilepsy (Scassellati et al. 2020). Furthermore, VPA was reported to decrease serum zinc (Doboszewska et al. 2019; Jia et al. 2020). Here, serum zinc increased either after acute or chronic administration of $ZnCl_2$ but not after treatment with TC-G 1008, which is consistent with the observation that plasma zinc responds to zinc supplementation (King et al. 2015) and with a previous study which did not show changes in serum zinc concentration after a 2-week administration of TC-G 1008 (Starowicz et al. 2019).

In summary, the effects of TC-G 1008 in acute seizure models in mice or zebrafish may be attributable to its action at GPR39 or, presumably, 5HT1A, but our data consistently support the hypothesis that activation of GPR39 aggravated epileptogenesis in the PTZ-kindling model. Our data argue against GPR39 activation being a therapeutic strategy for treating epilepsy and raise the possibility that antagonists of GPR39 shall be tested as antiepileptogenic drugs.

Potential worsened outcome of epilepsies may be considered when designing drugs for other diseases which mechanism of action will be GPR39 agonism. We showed that the behavioral effects of TC-G 1008 on epileptogenesis induced by PTZ are mediated by the GPR39 receptor, but we concomitantly demonstrated that the effects on CREB activation in the hippocampus may be induced by other targets, thereby showing for the first time the non-selective activity of TC-G 1008 in animal brain tissue. The possibility of non-selective activity of this small molecule agonist was previously indicated by *in vitro* data (Sato et al. 2016). Based on the analysis of the downstream effects of TC-G 1008 in the hippocampus GPR39 KO mice we suggest a critical reassessment of the existing literature, as some of the effects previously attributed to TC-G 1008 action at GPR39 may have arisen from different mechanisms.

Statements & Declarations

Funding: The study was supported by a grant from the National Science Centre, Poland (2016/20/S/NZ7/00424).

Competing interests: The authors have no relevant financial or non-financial interests to disclose.

Author contributions: All authors contributed to the study conception and design. Material preparation, data collection and analysis were performed by Urszula Doboszewska, Katarzyna Socała, Mateusz Pieróg, Dorota Nieoczym, Jan Sawicki, Małgorzata Szafarz, Kinga Gawel, Anna Rafalo-Ulińska, Adam Sajnóg, Elżbieta Wyska, Camila V. Esguerra, Bernadeta Szewczyk, Ireneusz Sowa, Piotr Wlaź. The first draft of the manuscript was written by Urszula Doboszewska and all authors commented on previous versions of the manuscript. All authors read and approved the final manuscript.

Data availability: The data that support the findings of this study are available from the corresponding author upon reasonable request.

Ethics approval: Housing and experimental procedures were conducted in accordance with the European Union Directive of 22 September 2010 (2010/63/EU) and Polish and Norwegian legislation acts concerning animal experimentation. The experiments in mice were approved by the Local Ethical Committee in Lublin (experiments in non-genetically modified mice: approval numbers 38/2017, 48/2018, 110/2018, 36/2019; experiments in GPR39 KO mice: approval numbers 72/2019, 16/2020), and the I Local Ethical Committee in Warsaw (approval number 811/2019 regarding generation of the GPR39 KO mouse line). The experiments in zebrafish were approved by the Norwegian Food Safety Authority experimental animal administration's supervisory and application system (“Forsøksdyrforvatningen tilsyns- og søknadssystem”; FOTS ID 15469 and 23935).

References

Afrikanova T, Serruys AS, Buenafe OE, Clinckers R, Smolders I, de Witte PA, Crawford AD, Esguerra CV (2013) Validation of the zebrafish pentylenetetrazol seizure model: locomotor versus electrographic responses to antiepileptic drugs. PLoS One 8:e54166

Alker W, Schwerdtle T, Schomburg L, Haase H (2019) A zinpyr-1-based fluorimetric microassay for free zinc in human serum. Int J Mol Sci 20:4006

Bassilana F, Carlson A, DaSilva JA, Grosshans B, Vidal S, Beck V, Wilmeringwetter B, Llamas LA, Showalter TB, Rigollier P, Bourret A, Ramamurthy A, Wu X, Harbinski F, Plonsky S, Lee L, Ruffner H, Grandi P, Schirle M, Jenkins J, Sailer AW, Bouwmeester T, Porter JA, Myer V, Finan PM, Tallarico JA, Kelleher JF, III, Seuwen K, Jain RK, Luchansky SJ (2014) Target identification for a Hedgehog pathway inhibitor reveals the receptor GPR39. Nat Chem Biol 10:343-349

Carpenter MC, Palmer AE (2017) Native and engineered sensors for Ca^{2+} and Zn^{2+}: lessons from calmodulin and MTF1. Essays Biochem 61:237-243

Chen NN, Zhao DJ, Sun YX, Wang DD, Ni H (2019) Long-term effects of zinc deficiency and zinc supplementation on developmental seizure-induced brain damage and the underlying GPR39/ZnT-3 and MBP expression in the hippocampus. Front Neurosci 13:920

Cole TB, Robbins CA, Wenzel HJ, Schwartzkroin PA, Palmiter RD (2000) Seizures and neuronal damage in mice lacking vesicular zinc. Epilepsy Res 39:153-169

Davis CM, Bah TM, Zhang WH, Nelson JW, Golgotiu K, Nie X, Alkayed FN, Young JM, Woltjer RL, Silbert LC, Grafe MR, Alkayed NJ (2021) GPR39 localization in the aging human brain and correlation of expression and polymorphism with vascular cognitive impairment. Alzheimers Dement (N Y) 7:e12214

Doboszewska U, Mlyniec K, Wlaz A, Poleszak E, Nowak G, Wlaz P (2019) Zinc signaling and epilepsy. Pharmacol Ther 193:156-177

Fisher RS, Acevedo C, Arzimanoglou A, Bogacz A, Cross JH, Elger CE, Engel J, Jr., Forsgren L, French JA, Glynn M, Hesdorffer DC, Lee BI, Mathern GW, Moshe SL, Perucca E, Scheffer IE, Tomson T, Watanabe M, Wiebe S (2014) ILAE official report: a practical clinical definition of epilepsy. Epilepsia 55:475-482

Fjellstrom O, Larsson N, Yasuda S, Tsuchida T, Oguma T, Marley A, Wennberg-Huldt C, Hovdal D, Fukuda H, Yoneyama Y, Sasaki K, Johansson A, Lundqvist S, Brengdahl J, Isaacs RJ, Brown D, Geschwindner S, Benthem L, Priest C, Turnbull A (2015) Novel Zn^{2+} modulated GPR39 receptor agonists do not drive acute insulin secretion in rodents. PLoS One 10:e0145849

Fountain NB (2000) Status epilepticus: risk factors and complications. Epilepsia 41 Suppl 2:S23-S30

Frimurer TM, Mende F, Graae AS, Engelstoft MS, Egerod KL, Nygaard R, Gerlach LO, Hansen JB, Schwartz TW, Holst B (2017) Model-based discovery of synthetic agonists for the Zn^{2+}-sensing G-protein-coupled receptor 39 (GPR39) reveals novel biological functions. J Med Chem 60:886-898

Galanopoulou AS, Buckmaster PS, Staley KJ, Moshe SL, Perucca E, Engel J, Jr., Loscher W, Noebels JL, Pitkanen A, Stables J, White HS, O'Brien TJ, Simonato M (2012) Identification of new epilepsy treatments: issues in preclinical methodology. Epilepsia 53:571-582

Gawel K, Langlois M, Martins T, van der Ent W, Tiraboschi E, Jacmin M, Crawford AD, Esguerra CV (2020) Seizing the moment: zebrafish epilepsy models. Neurosci Biobehav Rev 116:1-20

Gilad D, Shorer S, Ketzef M, Friedman A, Sekler I, Aizenman E, Hershfinkel M (2015) Homeostatic regulation of KCC2 activity by the zinc receptor mZnR/GPR39 during seizures. Neurobiol Dis 81:4-13

Goldberg EM, Coulter DA (2013) Mechanisms of epileptogenesis: a convergence on neural circuit dysfunction. Nat Rev Neurosci 14:337-349

Grabrucker AM, Schmeisser MJ, Udvardi PT, Arons M, Schoen M, Woodling NS, Andreasson KI, Hof PR, Buxbaum JD, Garner CC, Boeckers TM (2011) Amyloid beta protein-induced zinc sequestration leads to synaptic loss via dysregulation of the ProSAP2/Shank3 scaffold. Mol Neurodegener 6:65

Grunddal KV, Diep TA, Petersen N, Tough IR, Skov LJ, Liu L, Buijink JA, Mende F, Jin C, Jepsen SL, Sorensen LME, Achiam MP, Strandby RB, Bach A, Hartmann B, Frimurer TM, Hjorth SA, Bouvier M, Cox H, Holst B (2021) Selective release of gastrointestinal hormones induced by an orally active GPR39 agonist. Mol Metab 49:101207

Gutierrez-Ruiz JR, Villafana S, Ruiz-Hernandez A, Viruette-Pontigo D, Menchaca-Cervantes C, Aguayo-Ceron KA, Huang F, Hong E, Romero-Nava R (2022) Expression profiles of GPR21, GPR39, GPR135, and GPR153 orphan receptors in different cancers. Nucleosides Nucleotides Nucleic Acids 41:123-136

Hauser AS, Attwood MM, Rask-Andersen M, Schioth HB, Gloriam DE (2017) Trends in GPCR drug discovery: new agents, targets and indications. Nat Rev Drug Discov 16:829-842

Hershfinkel M, Kandler K, Knoch ME, Dagan-Rabin M, Aras MA, Abramovitch-Dahan C, Sekler I, Aizenman E (2009) Intracellular zinc inhibits KCC2 transporter activity. Nat Neurosci 12:725-727

Hershfinkel M, Moran A, Grossman N, Sekler I (2001) A zinc-sensing receptor triggers the release of intracellular Ca^{2+} and regulates ion transport. Proc Natl Acad Sci U S A 98:11749-11754

Holst B, Egerod KL, Schild E, Vickers SP, Cheetham S, Gerlach LO, Storjohann L, Stidsen CE, Jones R, Beck-Sickinger AG, Schwartz TW (2007) GPR39 signaling is stimulated by zinc ions but not by obestatin. Endocrinology 148:13-20

Iovino L, Cooper K, deRoos P, Kinsella S, Evandy C, Ugrai T, Mazziotta F, Ensbey KS, Granadier D, Hopwo K, Smith C, Gagnon A, Galimberti S, Petrini M, Hill GR, Dudakov JA (2022) Activation of the zinc-sensing receptor GPR39 promotes T-cell reconstitution after hematopoietic cell transplant in mice. Blood 139:3655-3666

Iqbal R, Jain GK, Siraj F, Vohora D (2018) Aromatase inhibition by letrozole attenuates kainic acid-induced seizures but not neurotoxicity in mice. Epilepsy Res 143:60-69

Iughetti L, Lucaccioni L, Fugetto F, Predieri B, Berardi A, Ferrari F (2018) Brain-derived neurotrophic factor and epilepsy: a systematic review. Neuropeptides 72:23-29

Jia W, Song Y, Yang L, Kong J, Boczek T, He Z, Wang Y, Zhang X, Hu H, Shao D, Tang H, Xia L, Xu X, Guo F (2020) The changes of serum zinc, copper, and selenium levels in epileptic patients: a systematic review and meta-analysis. Expert Rev Clin Pharmacol 13:1047-1058

Khan MZ (2016) A possible significant role of zinc and GPR39 zinc sensing receptor in Alzheimer disease and epilepsy. Biomed Pharmacother 79:263-272

Khanam R, Vohora D (2021) Protocol for 6 Hz corneal stimulation in rodents for refractory seizures. In: Vohora D (ed) Experimental and translational methods to screen drugs effective against seizures and epilepsy, Springer, New York, NY, USA, pp 167-179

Kimball AW, Burnett WT, Jr., Doherty DG (1957) Chemical protection against ionizing radiation. I. Sampling methods for screening compounds in radiation protection studies with mice. Radiat Res 7:1-12

King JC, Brown KH, Gibson RS, Krebs NF, Lowe NM, Siekmann JH, Raiten DJ (2015) Biomarkers of nutrition for development (BOND)-zinc review. J Nutr 146:858S-885S

Laitakari A, Liu L, Frimurer TM, Holst B (2021) The zinc-sensing receptor GPR39 in physiology and as a pharmacological target. Int J Mol Sci 22:3872

Lee JY, Cole TB, Palmiter RD, Koh JY (2000) Accumulation of zinc in degenerating hippocampal neurons of ZnT3-null mice after seizures: evidence against synaptic vesicle origin. J Neurosci 20:RC79

Lin TW, Harward SC, Huang YZ, McNamara JO (2020) Targeting BDNF/TrkB pathways for preventing or suppressing epilepsy. Neuropharmacology 167:107734

Loscher W (2021) Models of seizures and epilepsy: important tools in the discovery and evaluation of novel epilepsy therapies. In: Vohora D (ed) Experimental and translational methods to screen drugs effective against seizures and epilepsy, Springer, New York, NY, USA, pp 3-7

Maret W (2001) Crosstalk of the group IIa and IIb metals calcium and zinc in cellular signaling. Proc Natl Acad Sci U S A 98:12325-12327

Maret W (2017) Zinc in cellular regulation: the nature and significance of "zinc signals". Int J Mol Sci 18:2285

Mertz C, Krarup S, Jensen CD, Lindholm SEH, Kjaer C, Pinborg LH, Bak LK (2020) Aspects of cAMP signaling in epileptogenesis and seizures and its potential as drug target. Neurochem Res 45:1247-1255

Methner C, Cao Z, Mishra A, Kaul S (2021) Mechanism and potential treatment of the "no reflow" phenomenon after acute myocardial infarction: role of pericytes and GPR39. Am J Physiol Heart Circ Physiol 321:H1030-H1041

Mlyniec K, Siodlak D, Doboszewska U, Nowak G (2021) GPCR oligomerization as a target for antidepressants: focus on GPR39. Pharmacol Ther 225:107842

Mlyniec K, Starowicz G, Gawel M, Frackiewicz E, Nowak G (2016) Potential antidepressant-like properties of the TC G-1008, a GPR39 (zinc receptor) agonist. J Affect Disord 201:179-184

Moore AN, Waxham MN, Dash PK (1996) Neuronal activity increases the phosphorylation of the transcription factor cAMP response element-binding protein (CREB) in rat hippocampus and cortex. J Biol Chem 271:14214-14220

Moore YE, Kelley MR, Brandon NJ, Deeb TZ, Moss SJ (2017) Seizing control of KCC2: a new therapeutic target for epilepsy. Trends Neurosci 40:555-571

Nieoczym D, Socala K, Gawel K, Esguerra CV, Wyska E, Wlaz P (2019) Anticonvulsant activity of pterostilbene in zebrafish and mouse acute seizure tests. Neurochem Res 44:1043-1055

Peukert S, Hughes R, Nunez J, He G, Yan Z, Jain R, Llamas L, Luchansky S, Carlson A, Liang G, Kunjathoor V, Pietropaolo M, Shapiro J, Castellana A, Wu X, Bose A (2014) Discovery of 2-pyridylpyrimidines as the first orally bioavailable GPR39 agonists. ACS Med Chem Lett 5:1114-1118

Potschka H (2021) Procedures for electrical and chemical kindling models in rats and mice. In: Vohora D (ed) Experimental and translational methods to screen drugs effective against seizures and epilepsy, Springer, New York, NY, USA, pp 103-119

Sah A, Kharitonova M, Mlyniec K (2021) Neuronal correlates underlying the role of the zinc sensing receptor (GPR39) in passive-coping behaviour. Neuropharmacology 198:108752

Salaciak K, Pytka K (2021) Biased agonism in drug discovery: is there a future for biased 5-HT_{1A} receptor agonists in the treatment of neuropsychiatric diseases? Pharmacol Ther 227:107872

Satala G, Duszynska B, Stachowicz K, Rafalo A, Pochwat B, Luckhart C, Albert PR, Daigle M, Tanaka KF, Hen R, Lenda T, Nowak G, Bojarski AJ, Szewczyk B (2016) Concentration-dependent dual mode of Zn action at serotonin 5-HT_{1A} receptors: in vitro and in vivo studies. Mol Neurobiol 53:6869-6881

Sato S, Huang XP, Kroeze WK, Roth BL (2016) Discovery and characterization of novel GPR39 agonists allosterically modulated by zinc. Mol Pharmacol 90:726-737

Scassellati C, Bonvicini C, Benussi L, Ghidoni R, Squitti R (2020) Neurodevelopmental disorders: metallomics studies for the identification of potential biomarkers associated to diagnosis and treatment. J Trace Elem Med Biol 60:126499

Schauwecker PE (2011) The relevance of individual genetic background and its role in animal models of epilepsy. Epilepsy Res 97:1-11

Socala K, Doboszewska U, Wlaz P (2020) Salvinorin A does not affect seizure threshold in mice. Molecules 25:1204

Socala K, Mogilski S, Pierog M, Nieoczym D, Abram M, Szulczyk B, Lubelska A, Latacz G, Doboszewska U, Wlaz P, Kaminski K (2019) KA-11, a novel pyrrolidine-2,5-dione derived

broad-spectrum anticonvulsant: its antiepileptogenic, antinociceptive properties and in vitro characterization. ACS Chem Neurosci 10:636-648

Socala K, Nieoczym D, Pierog M, Wyska E, Szafarz M, Doboszewska U, Wlaz P (2018) Effect of tadalafil on seizure threshold and activity of antiepileptic drugs in three acute seizure tests in mice. Neurotox Res 34:333-346

Socala K, Wlaz P (2021) Acute seizure tests used in epilepsy research: step-by-step protocol of the maximal electroshock seizure (MES) test, the maximal electroshock seizure threshold (MEST) test, and the pentylenetetrazole (PTZ)-induced seizure test in rodents. In: Vohora D (ed) Experimental and translational methods to screen drugs effective against seizures and epilepsy, Springer, New York, NY, USA, pp 79-102

Starowicz G, Jarosz M, Frackiewicz E, Grzechnik N, Ostachowicz B, Nowak G, Mlyniec K (2019) Long-lasting antidepressant-like activity of the GPR39 zinc receptor agonist TC-G 1008. J Affect Disord 245:325-334

Thom M (2014) Review: Hippocampal sclerosis in epilepsy: a neuropathology review. Neuropathol Appl Neurobiol 40:520-543

van Loo KM, Schaub C, Pitsch J, Kulbida R, Opitz T, Ekstein D, Dalal A, Urbach H, Beck H, Yaari Y, Schoch S, Becker AJ (2015) Zinc regulates a key transcriptional pathway for epileptogenesis via metal-regulatory transcription factor 1. Nat Commun 6:8688

Wang G, Zhu Z, Xu D, Sun L (2020) Advances in understanding CREB signaling-mediated regulation of the pathogenesis and progression of epilepsy. Clin Neurol Neurosurg 196:106018

Wasilewska I, Gupta RK, Wojtas B, Palchevska O, Kuznicki J (2020) stim2b knockout induces hyperactivity and susceptibility to seizures in zebrafish larvae. Cells 9:1285

Xie S, Jiang X, Doycheva DM, Shi H, Jin P, Gao L, Liu R, Xiao J, Hu X, Tang J, Zhang L, Zhang JH (2021) Activation of GPR39 with TC-G 1008 attenuates neuroinflammation via SIRT1/PGC-1a/Nrf2 pathway post-neonatal hypoxic-ischemic injury in rats. J Neuroinflammation 18:226-02289

Yasuda S, Miyazaki T, Munechika K, Yamashita M, Ikeda Y, Kamizono A (2007) Isolation of Zn^{2+} as an endogenous agonist of GPR39 from fetal bovine serum. J Recept Signal Transduct Res 27:235-246

Supplementary Files

This is a list of supplementary files associated with this preprint. Click to download.

- ver2suppl.pdf